Synthesis, Structure, and Reactivity of sp Carbon Chains with Bis(phosphine) Pentafluorophenylplatinum Endgroups: Butadiynediyl (C_4) through Hexadecaoctaynediyl (C_{16}) Bridges, and Beyond

Wolfgang Mohr, Jürgen Stahl, Frank Hampel, and J. A. Gladysz*[a]

Abstract: The reaction of *trans*-[$(C_6F_5)(p\text{-tol}_3P)_2PtCl$] (**PtCl**) and butadiyne (cat. CuI, $HNEt_2$) gives *trans*-[$(C_6F_5)(p\text{-tol}_3P)_2Pt(C{\equiv}C)_2H$] (**$PtC_4H$**, 81%), which reacts with excess $HC{\equiv}CSiEt_3$ under Hay coupling conditions (O_2, cat. CuCl/TMEDA, acetone) to yield **PtC_6Si** (53%). A solution of **PtC_6Si** in acetone is treated with wet nBu$_4$NF to generate **PtC_6H**. The addition of $ClSiMe_3$ (F^- scavenger) and then excess $HC{\equiv}CSiEt_3$ under Hay conditions gives **PtC_8Si** (39%). Hay homocouplings of **PtC_4H**, **PtC_6H**, and **PtC_8H** (generated in situ analogously to **PtC_6H**) yield **PtC_8Pt**, **$PtC_{12}Pt$**, and **$PtC_{16}Pt$** (97–92%). Reactions of **PtC_4H** and **PtC_6H** with **PtCl** (cat. CuCl, $HNEt_2$) give **PtC_4Pt** and **PtC_6Pt** (69%, 34%). The attempted conversion of **PtC_8H** to **$PtC_{10}Si$** affords mainly **$PtC_{16}Pt$**, with traces of **$PtC_{20}Pt$** and **$PtC_{24}Pt$**. The complexes **PtC_xPt** are exceedingly stable (dec pts 234 to 288 °C), and Et_3P displaces p-tol$_3$P to give the corresponding compounds **Pt′C_8Pt′** and **Pt′C_{12}Pt′** (94–90%). The effect of carbon chain lengths upon IR $\nu_{C\equiv C}$ patterns (progressively more bands), UV/Vis spectra (progressively red-shifted and more intense bands with $\varepsilon > 600\,000\,M^{-1}cm^{-1}$), redox properties (progressively more difficult and less reversible oxidations), and NMR values are studied, and analyzed with respect to the polymeric sp carbon allotrope "carbyne". The crystal structure of **$PtC_{12}Pt$** shows a dramatic, unprecedented degree of chain bending, whereas the chains in **PtC_8Pt**, **Pt′C_{12}Pt′**, and **$PtC_{16}Pt$** are nearly linear.

Keywords: carbyne · crystal structures · oxidative coupling · platinum · polyynes

Introduction

There has been extensive recent interest in the synthesis and study of compounds composed of long sp carbon chains and transition-metal endgroups, $L_nMC_xML_n$.[1–12] These efforts have been motivated by a number of fundamental and applied objectives. For example, metal fragments provide dramatic stability enhancements over hydrogen or *n*-alkyl endgroups, facilitating characterization of basic properties. At shorter chain lengths, such compounds provide models for oligoynes believed to occur in interstellar clouds and carbon-rich stars.[13] At longer chain lengths, models for the polymeric sp carbon allotrope "carbyne",[14] the one-dimensional counterpart of graphite and diamond, are realized. Complexes in which metals are bridged by unsaturated ligands also exhibit a rich variety of redox and charge- or energy-transfer phenomena, and are under investigation as components in molecular-scale devices.[15] An sp carbon chain constitutes the most fundamental and wirelike connecting group, and cannot be twisted out of conjugation.

In terms of current art, C_8 complexes represent a logical dividing line between "short" and "long" carbon chains. Approximately thirty such species have now been reported, all with identical endgroups and polyynediyl or $-(C{\equiv}C)_n-$ bridges, as represented by **I** in Scheme 1.[2–11] In principle, two consecutive one-electron oxidations can give related dicationic complexes with cumulenic or $=(C{=}C)_n=$ bridges (**III**). Cyclic voltammograms sometimes show reversible couples,[2, 7, 8] and several such C_4 complexes have been isolated. However, the C_8 analogues are distinctly less stable, and have not yet proved spectroscopically observable. One diiron C_8 cation radical, representing the intermediate oxidation state **II**, has proved isolable.[2a] As illustrated in Scheme 1, three classes of complexes with longer chains have been reported: chiral dirhenium C_{12}, C_{16}, and C_{20} complexes of the type **1**, the properties of which have been summarized in a detailed full paper;[7] Akita's diiron C_{12} complex **2**;[4b] diplatinum C_{12} and C_{16} complexes of the type **3** and analogues with pentafluorophenyl ligands, as described in two preliminary communications.[9, 10] Similar nonmetallic C_x species with trialkylsilyl, cyano, and bulky, dendrimer-like aryl endgroups have also proved isolable.[16, 17]

[a] Prof. Dr. J. A. Gladysz, Dr. W. Mohr, Dipl.-Chem. J. Stahl, Dr. F. Hampel
Institut für Organische Chemie
Friedrich-Alexander-Universität Erlangen-Nürnberg
Henkestraße 42, 91054 Erlangen (Germany)
Fax: (+49) 9131-8526865
E-mail: gladysz@organik.uni-erlangen.de

DOI: 10.1002/chem.200204741

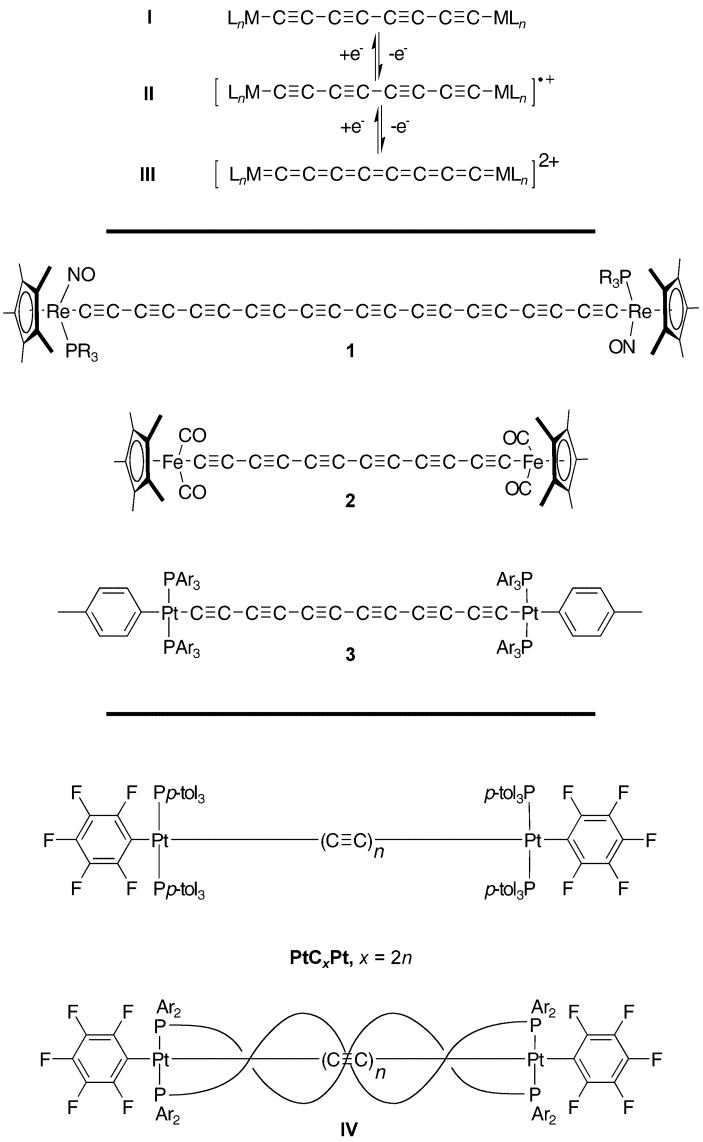

Scheme 1. Metal complexes of long sp carbon chains: selected redox possibilities (**I**–**III**), specific examples (**1**–**3**), and target molecules (**PtC$_x$Pt**).

Herein, we describe the synthesis, structure, reactivity, and detailed spectroscopic characterization of a series of C_x complexes ($x = 4$, 6, 8, 12, 16, 20, 24) with sixteen-valence-electron, pentafluorophenyl-substituted platinum endgroups. These are designated **PtC$_x$Pt**, as defined in Scheme 1. The effect of chain length upon thermal stabilities and IR, NMR, UV/Vis, and redox properties is carefully documented, with **PtC$_{24}$Pt** representing the longest sp carbon chain complex prepared to date. These data complement those obtained for dirhenium complexes of the type **1**, which feature eighteen-valence-electron endgroups,[7] and together with those for all known series of C_x compounds help to define the properties of the polymeric carbon allotrope carbyne. The complexes **PtC$_x$Pt** are also the first species of the type **I** to be used as functional building blocks for more complex structures. As recently communicated,[11] coordination-driven self-assembly can be employed to "insulate" the $(C\equiv C)_n$ moiety by two sp^3 carbon chains, which adopt a double helical motif as shown in **IV** (Scheme 1). Hence, a further purpose of this study is to provide the baseline data required to define the effect of this "insulation" on chemical and physical properties.

Results

Syntheses of PtC$_x$H/Si complexes: For reasons described elsewhere,[11] we sought a series of compounds with platinum endgroups more Lewis acidic than in **3** (Scheme 1). Accordingly, we wondered if the *p*-tolyl ligand could be replaced by a pentafluorophenyl ligand. Our attention was drawn to the latter as a result of its extensively developed platinum chemistry, pioneered largely by groups in Zaragoza.[18–20] The tetrahydrothiophene (THT) derivative $[\{(C_6F_5)(tht)Pt(\mu\text{-}Cl)\}_2]$[19, 21] had previously been shown to react with various donor ligands to give complexes of the formula *trans*-$[(C_6F_5)(L)_2PtCl]$.[20, 22] As shown in Scheme 2, an analogous reaction with *p*-tol$_3$P gave *trans*-$[(C_6F_5)(p\text{-tol}_3P)_2PtCl]$ (**PtCl**) in 93% yield after workup.

We next sought to replace the chlorine ligand in **PtCl** by a butadiynyl group. A method previously applied en route to **3** and related compounds (excess butadiyne, cat. CuI, $HNEt_2$),[10] gave *trans*-$[(C_6F_5)(p\text{-tol}_3P)_2Pt(C\equiv C)_2H]$ (**PtC$_4$H**) in 81% yield (Scheme 2). All stable new complexes isolated in sufficient quantity were characterized by IR and NMR (^{1}H, ^{13}C, ^{31}P) spectroscopy, mass spectrometry, and microanalysis, as well as by additional means described below. Complexes **PtCl** and **PtC$_4$H**, and all subsequently derived compounds, showed one ^{31}P NMR signal, and virtual coupling patterns typical of *trans* square-planar bis(phosphine) species.[23]

One of the major challenges associated with syntheses of "higher" $L_nMC_xML_n$ complexes is efficient chain extension.[6] We were therefore curious whether longer $H(C\equiv C)_nH$ building blocks might be employed. Since these present greater explosion hazards than butadiyne,[24] we attempted their generation in situ from the corresponding bis(trimethylsilyl) compounds $TMS(C\equiv C)_nTMS$ ($n = 3, 4$)[25, 26] with wet nBu$_4$NF in acetone at $-78\,^\circ$C. However, various problems soon became apparent. First, these compounds required several steps to prepare (direct precursors of butadiyne are commercially available). Second, the initial products **PtC$_x$H** were much more labile than **PtC$_4$H**, as observed for other types of $L_nM(C\equiv C)_nH$ complexes[7, 9] and further documented below. Third, mixtures of **PtC$_x$H**, **PtC$_x$TMS**, and **PtC$_x$Pt** were

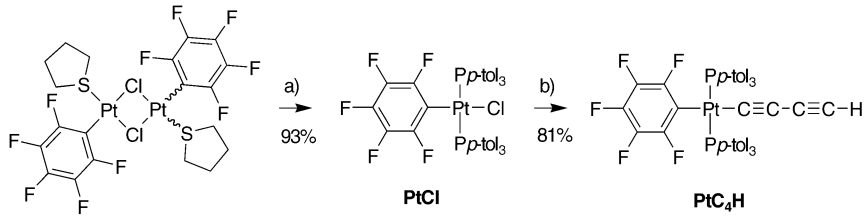

Scheme 2. Platinum endgroup synthesis. a) *p*-tol$_3$P; b) butadiyne, cat. CuI, $HNEt_2$.

commonly obtained, even when excess **PtCl** was employed. We therefore abandoned this approach in favor of simple iterative chain extensions, as summarized by the reactions presented vertically in Scheme 3.

Thus, **PtC_4H** and an excess of the commercially available silylated ethyne $HC{\equiv}CSiEt_3$ were allowed to react under Hay oxidative coupling conditions (excess O_2, 0.20–0.25 equiv CuCl/tetramethylethylenediamine (TMEDA)) in refluxing acetone.[27] Workup gave the desired cross-coupled silylated hexatriynyl complex **PtC_6Si** in 53% yield, as well as some homocoupling product **PtC_8Pt** (25%; see below). A subsequent reaction with nBu$_4$NF in wet THF gave the parent hexatriynyl complex **PtC_6H** as a white powder in 85% yield after a low-temperature workup. This material darkened within a few minutes at room temperature, but was stable at $-18\,^{\circ}C$ for several days. Spectroscopic data are summarized with those of other complexes below.

To minimize the handling of **PtC_6H**, coupling conditions were sought that would allow it (and higher homologues) to be generated in situ. Thus, a solution of **PtC_6Si** in *acetone* was treated with nBu$_4$NF in wet THF to generate **PtC_6H**. Then $ClSiMe_3$ was added, and the Hay coupling with excess $HC{\equiv}CSiEt_3$ repeated. Chromatography gave the silylated octatetraynyl complex **PtC_8Si** (Scheme 3) in 39% yield. When $ClSiMe_3$ was omitted, only traces of **PtC_8Si** formed. We hypothesize that the $ClSiMe_3$ scavenges fluoride ions, which for some reason interfere with the coupling. The modest yield of **PtC_8Si** is ameliorated by a useful by-product, **$PtC_{12}Pt$** (ca. 25%).

A $CDCl_3$ solution of **PtC_8Si** and nBu$_4$NF in wet THF was combined in a NMR tube at room temperature. IR and NMR (^{1}H, ^{31}P) spectra verified the clean formation of **PtC_8H**, which showed no decomposition over the course of 1 h. However, samples rapidly decomposed when concentrated. Finally, similar attempts were made to cross-couple **PtC_4H** and **PtC_6H** with diynes such as $HC{\equiv}CC{\equiv}CSiMe_3$. Although such four-carbon chain extensions would greatly enhance synthetic efficiency, only very low yields of the target molecules were realized.

Syntheses of PtC_8Pt, $PtC_{12}Pt$, and $PtC_{16}Pt$: The homocouplings presented horizontally in Scheme 3 were investigated next. The reaction of **PtC_4H** under Hay conditions in refluxing acetone gave the C_8 or μ-octatetraynediyl complex **PtC_8Pt** in 97% yield after workup. Acetone solutions of **PtC_6Si** and **PtC_8Si** were treated with nBu$_4$NF in wet THF to generate **PtC_xH** as above, followed by $ClSiMe_3$. Hay homocouplings were then effected in situ to give the μ-dodecahexaynediyl and μ-hexadecaoctaynediyl complexes **$PtC_{12}Pt$** and **$PtC_{16}Pt$** in 92% yields. Rates increased with increasing chain length, such that the synthesis of **$PtC_{16}Pt$** could be conducted at room temperature.[28] Small quantities of **$PtC_{16}Pt$** were also ob-

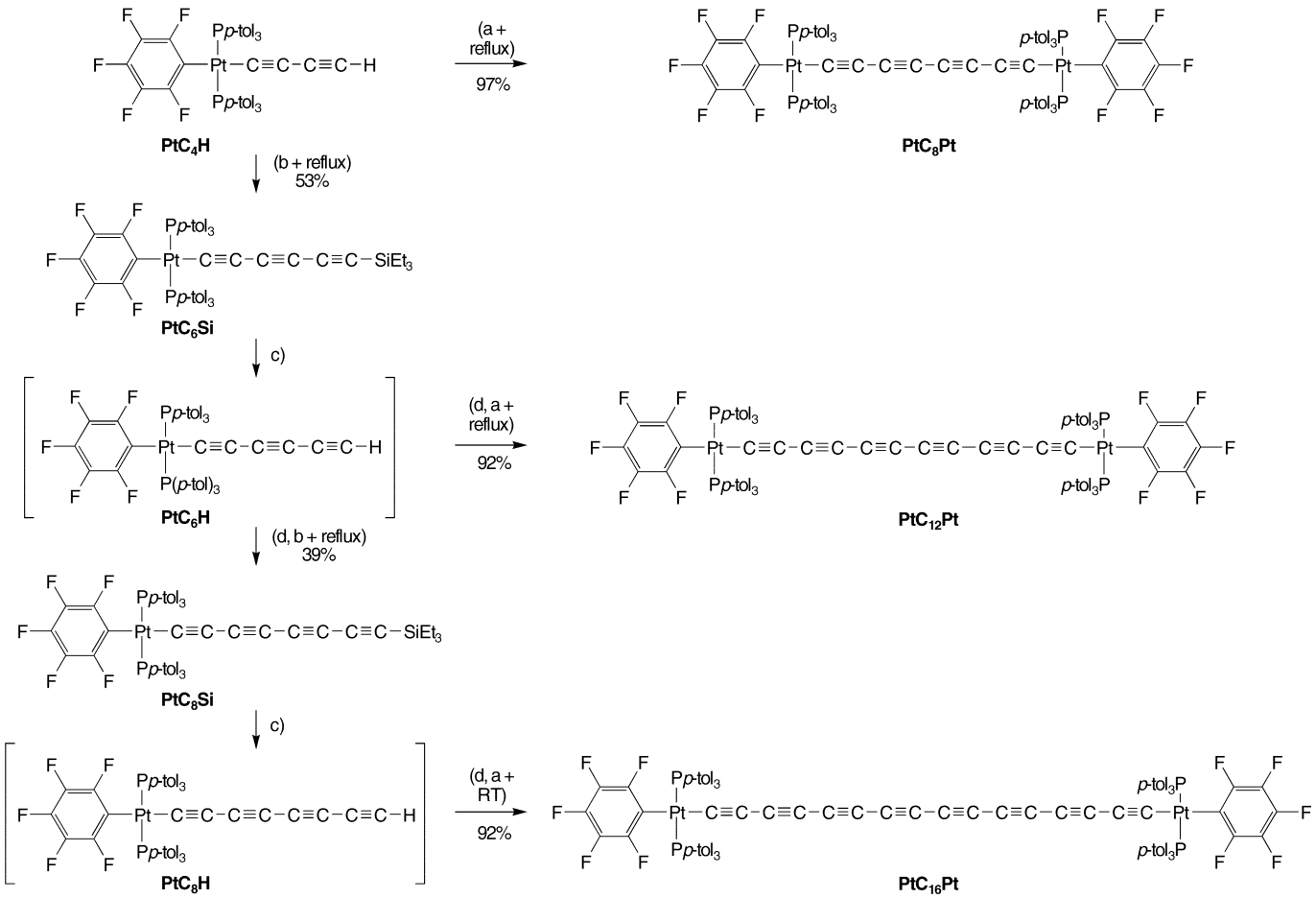

Scheme 3. Syntheses of **PtC_8Pt**, **$PtC_{12}Pt$**, and **$PtC_{16}Pt$**. a) O_2, cat. CuCl/TMEDA, acetone; b) $HC{\equiv}CSiEt_3$ (excess), O_2, cat. CuCl/TMEDA, acetone; c) wet nBu$_4$NF; d) $ClSiMe_3$.

tained by subjecting the **PtCl**/H(C≡C)$_4$H reaction mixtures described above to the Hay conditions. However, separation from the many by-products was tedious.

Complexes **PtC$_8$Pt**, **PtC$_{12}$Pt**, and **PtC$_{16}$Pt** were air-stable yellow to apricot powders of extraordinary thermal stability. As summarized in Table 1, decomposition points were $\geq 234\,^{\circ}C$. The complexes were highly soluble in common organic solvents, and showed progressively *shorter* retention times in silica gel chromatography. IR, NMR, and UV/Vis spectra were recorded under rigorously identical conditions. Key data are summarized in Table 2, Table 3 and Table 4 and Figure 1, and the various chain length effects are thoroughly interpreted below.

Syntheses of PtC$_4$Pt and PtC$_6$Pt: To better analyze certain properties of the preceding compounds, lower homologues were sought. In an initial approach to **PtC$_4$Pt**, **PtCl** and ethyne were combined under conditions analogous to those used for butadiyne in Scheme 2. However, reaction was much slower, perhaps due to the lower acidity of ethyne,[29] and only modest yields of **PtC$_2$H** were obtained. Analogous condensations of ethyne with bis(tri*alkyl*phosphine) platinum halides work well.[30] However, to our knowledge there are no reports of successful reactions with bis(tri*aryl*phosphine) species. In a parallel study, we found that the Hay homocoupling of bis(triethylphosphine) complex *trans*-[(C$_6$F$_5$)(Et$_3$P)$_2$PtC≡CH] (**Pt′C$_2$H**) proceeded in low yield.[31] Pronounced steric effects upon Eglinton homocouplings of rhenium ethynyl and

Table 1. Thermal stability data [°C].

Complex	Mass loss (onset), TGA	Decomposition (onset), capillary thermolysis[a]
PtC$_4$Pt	332	260[b]
PtC$_6$Pt	251	240[c]
PtC$_8$Pt	252	234[b,d]
PtC$_{12}$Pt	270	288[b,d]
PtC$_{16}$Pt	270	270[b,d]
PtC$_4$H	180	171[b,e]

[a] Sealed; conventional melting point apparatus. [b] Decomposition without melting. [c] Melting at 189 °C. [d] See text for additional IR data. [e] Liquifies at a slightly higher temperature.

Table 2. Selected IR and ^{31}P NMR data for PtC$_x$ complexes.

Complex	IR $\nu_{C\equiv C}$ [cm^{-1}][a]	^{31}P{^{1}H} NMR (δ)[b] [$^1J_{P,Pt}$, Hz]
PtC$_4$Pt	not observed	16.3 [2713]
PtC$_6$Pt	not observed	17.2 [2683]
PtC$_8$Pt	2152 s, 2011 m	17.6 [2654]
PtC$_{12}$Pt	2127 m, 2088 s, 1992 m	17.7 [2622]
PtC$_{16}$Pt	2154 w, 2088 w, 2054 s, 1984 m	18.0 [2609]
PtC$_4$H	2154 m[c]	17.6 [2655]
PtC$_6$H	2162 s, 2108 m, 2003 m[d]	18.0 [2627]
PtC$_6$Si	2150 s, 2023 m	17.9 [2636]
PtC$_8$H	2131 s, 2069 s, 2003 s[b,d]	17.8 [2622]
PtC$_8$Si	2131 m, 2088 s, 2065 sh, 2015 w	17.9 [2624]
Pt′C$_8$Pt′	2140 s, 1997 m	13.2 [2393]
Pt′C$_{12}$Pt′	2131 m, 2096 s, 1996 m	13.5 [2376]

[a] Powder film unless noted. [b] In $CDCl_3$. [c] $\nu_{C\equiv H} = 3320$ w. [d] $\nu_{C\equiv H} = 3296$ w.

Table 3. Selected ^{13}C NMR data for PtC$_x$ complexes.[a]

Complex	Pt*C*≡ [$^1J_{C,Pt}$, Hz]	PtC≡*C* [$^2J_{C,Pt}$, Hz]	PtC≡C*C*	Other
PtC$_4$Pt	86.4 [970]	104.0 [262]	–	–
PtC$_6$Pt	95.8	98.4	61.1	–
PtC$_8$Pt	100.6 [998]	96.7 [265]	64.1	58.1
PtC$_{12}$Pt	106.5	95.5	65.7	63.0, 61.0, 57.1
PtC$_{16}$Pt	109.1	95.0	66.7	64.9, 63.1, 61.5, 60.1, 56.8
PtC$_4$H	97.8 [990]	94.9 [266]	72.5	59.6
PtC$_6$Si	104.2	95.4	66.1	91.2 (CSi), 80.3 (*C*CSi), 55.9
PtC$_8$Si	106.3 [1000]	95.2 [264]	66.6	90.2 (CSi), 82.9 (*C*CSi), 64.1, 59.3, 56.3
Pt′C$_8$Pt′	103.4	91.1 [285]	63.9	57.6
Pt′C$_{12}$Pt′	108.1	90.6	65.7	63.0, 61.1, 56.7

[a] In $CDCl_3$. The absence of a $J_{C,Pt}$ value indicates the coupling was not observed.

Table 4. UV/Vis data for PtC$_x$ complexes.

Complex	Wavelength (nm) [ε (M^{-1}cm^{-1})]
PtC$_4$Pt[a]	330 [17000], 350 [13200]
PtC$_6$Pt[a]	315 [44000], 345 [15000], 358 [11000], 369 [9000]
PtC$_8$Pt[b]	294 [88000], 326 [126000], 356 [7000], 383 [6000], 414 [3000]
PtC$_{12}$Pt[b]	315 [101000], 336 [267000], 359 [432000]
PtC$_{16}$Pt[b]	290 [46000], 306 [42000], 326 [54000], 346 [151000], 369 [397000], 397 [602000]
PtC$_{20}$Pt[c]	322, 344, 366, 392, 422
PtC$_{24}$Pt[c]	388, 416, 446
Pt′C$_8$Pt′	271 [62000], 288 [118000], 314 [131000], 350 [4000], 378 [4000], 410 [2000]
Pt′C$_{12}$Pt′	305 [91200], 329 [205000], 349 [338000]
PtC$_4$H[d]	305 [5600]
PtC$_6$Si[b]	244 [116000], 249 [125000], 255 [131000], 261 [104000]
PtC$_8$Si[b]	255 [62000], 269 [65000], 287 [98000], 310 [73000]
SiC$_8$Si[e]	221 [35000], 232 [63000], 244 [138000], 256 [195000], 321 [140], 344 [150], 349 [190], 369 [100], 375 [110]

[a] 1.25×10^{-5} M in CH_2Cl_2. [b] 1.25×10^{-6} M in CH_2Cl_2. [c] Hexane/CH_2Cl_2 (89:11 v/v; see Figure 1). [d] 1.25×10^{-4} M in CH_2Cl_2. [e] Methanol, from reference [16a] (similar values in hexane).

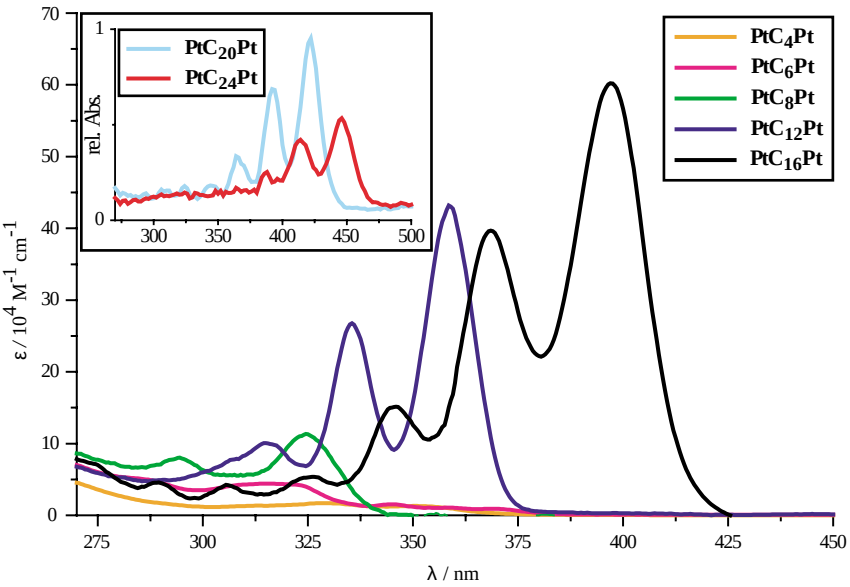

Figure 1. UV/Vis spectra of **PtC$_x$Pt** ($x = 4$, 6, 8, 12, 16) in CH_2Cl_2 and (inset) **PtC$_{20}$Pt** and **PtC$_{24}$Pt** in CH_2Cl_2/hexane (11:89 v/v).

butadiynyl complexes have been noted.[8a] Hence, this route to **PtC$_4$Pt** was abandoned.

The alternative shown in Scheme 4 was investigated next. The butadiynyl complex **PtC$_4$H** and a slight excess of **PtCl** were combined in the presence of $HNEt_2$ and a catalytic amount of CuCl. These conditions follow those used for the conversion of 1,3-butadiyne and **PtCl** to **PtC$_4$H** in Scheme 2, except with CuCl in place of CuI. No reaction occurred at room temperature. However, coupling took place over the course of 55 h at 50 °C, and workup gave **PtC$_4$Pt** in 69 % yield based upon the limiting reactant. When CuI was employed, a by-product formed that was difficult to separate, which was tentatively assigned as the iodide complex **PtI**.

Based upon this success, **PtC$_6$H** was generated in situ as described above and similarly combined with **PtCl**. Reaction now occurred at room temperature, and workup gave the target complex **PtC$_6$Pt** in 34 % yield. We attribute the lower yield to the lower stability of **PtC$_6$H**. Many other synthetic approaches were investigated, and gave much poorer results. Any conjugated polyyne with an odd number of triple bonds, such as **PtC$_6$Pt**, is of course not accessible by standard homocoupling reactions. Complexes **PtC$_4$Pt** and **PtC$_6$Pt** were, like their higher homologues, extremely stable, and key properties are incorporated into Table 1, Table 2, Table 3 and Table 4 and Figure 1 above.

Generation of PtC$_{20}$Pt and PtC$_{24}$Pt: We naturally wondered whether the above methodology could be extended to still longer carbon chains. As shown in Scheme 5, the elaboration of **PtC$_8$Si** to the silylated decapentaynyl complex **PtC$_{10}$Si** was attempted under conditions similar to those used for **PtC$_6$Si** to **PtC$_8$Si** in Scheme 3. To minimize the thermal decomposition of intermediate **PtC$_8$H**, the temperature was reduced to 25 – 40 °C. However, many products formed, which were partially separated by silica gel column chromatography. A minor component gave NMR data (^{1}H, ^{31}P) and a mass spectral molecular ion consistent with the target complex **PtC$_{10}$Si**. The major fraction consisted mainly of **PtC$_{16}$Pt**, but contained small amounts of several additional species.

Specifically, the mass spectrum of this fraction clearly exhibited a molecular ion for **PtC$_{20}$Pt**. A ^{31}P NMR spectrum showed three peaks, one for **PtC$_{16}$Pt** ($\delta = 18.0$ ppm) and the other two with plausible chemical shifts for **PtC$_{20}$Pt** and **PtC$_{24}$Pt** ($\delta = 17.9$ and 18.2 ppm; 77:15:8 ratio). The ^{13}C NMR and IR spectra also gave several new peaks (experimental section). The new species could be separated by analytical HPLC, and UV/Vis spectra were recorded using the detector (inset, Figure 1). Although extinction coefficients could not be measured, the patterns of long-wavelength bands provide convincing evidence for the formation of **PtC$_{20}$Pt** and **PtC$_{24}$Pt**. In view of the sub milligram quantities involved, no attempts were made to isolate pure samples. Possible mechanisms for these transformations are analyzed in the discussion section.

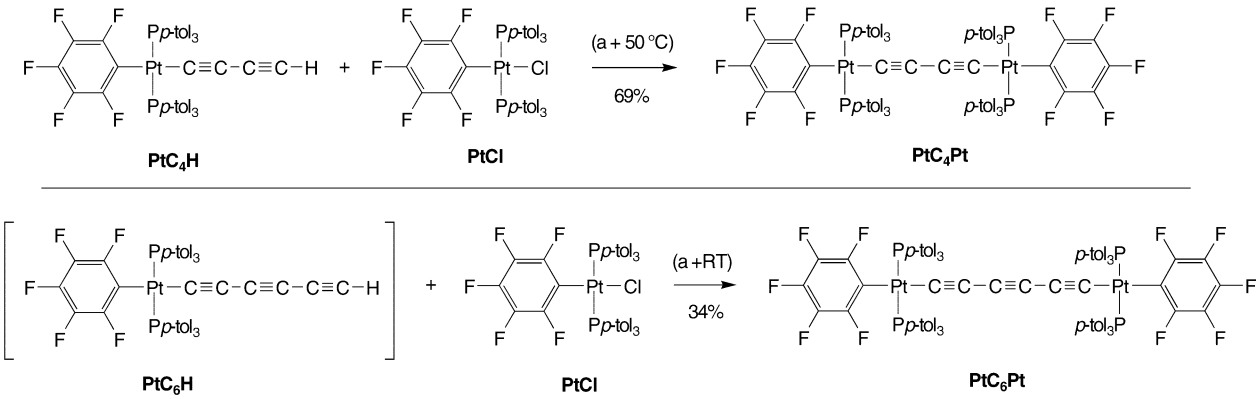

Scheme 4. Syntheses of **PtC$_4$Pt** and **PtC$_6$Pt**. a) cat. CuCl, $HNEt_2$.

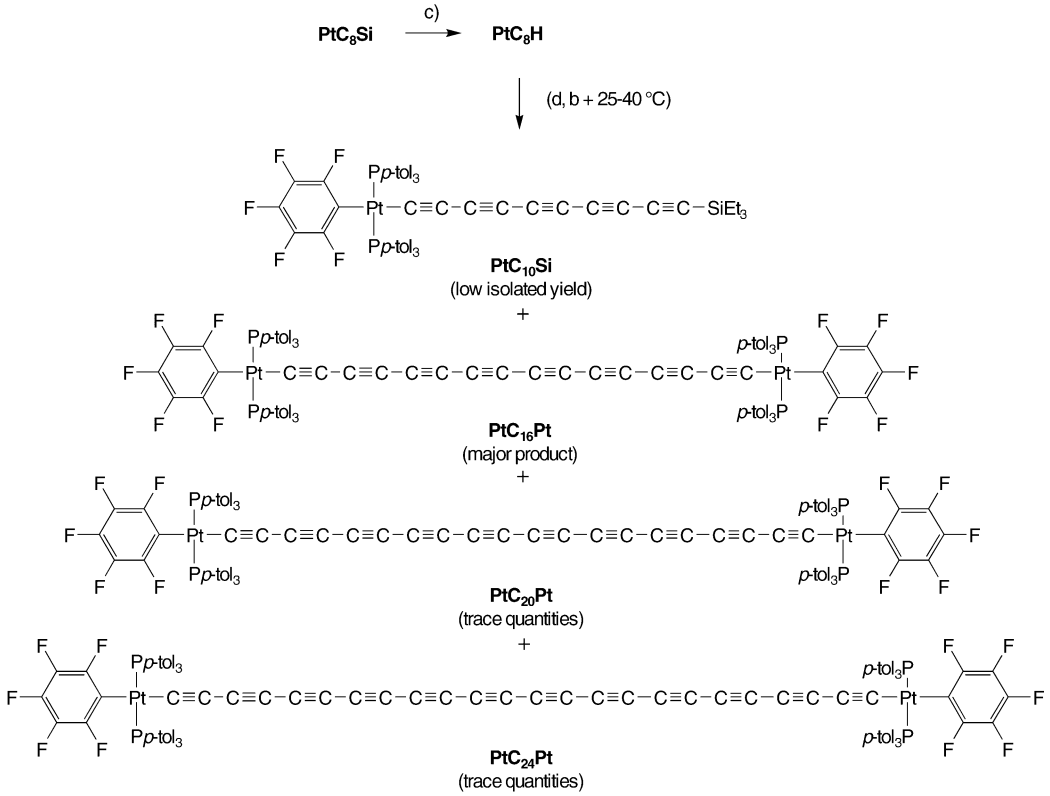

Scheme 5. Attempted extension of Scheme 3. b) $HC{\equiv}CSiEt_3$ (excess), O_2, cat. CuCl/TMEDA, acetone. c) wet nBu$_4$NF. d) $ClSiMe_3$.

Reactivity: We sought to probe three fundamental reactions of the title complexes: thermolysis, oxidation, and ligand substitution. The first has two aspects: how stable are the complexes, and do tractable products form? As summarized in Table 1, all were exceedingly stable, with decomposition points ranging from 234 to 288 °C. There was no sign of a diminution with chain length, and no explosions ever occurred. Except in the case of **PtC$_6$Pt**, which melted (189 °C), no pronounced endotherms or exotherms were observed by differential scanning calorimetry (DSC). Except for **PtC$_4$Pt**, thermogravimetric analysis (TGA) showed the onset of mass loss close to the decomposition point.

Next, several capillaries of **PtC$_8$Pt**, **PtC$_{12}$Pt**, or **PtC$_{16}$Pt** were simultaneously heated to just under the decomposition points, and then sequentially removed at approximately 10 °C intervals for IR analysis. In the case of **PtC$_8$Pt**, the IR $\nu_{C\equiv C}$ bands shifted slightly (230 °C, 2154/2011 cm^{-1}; 240 °C, 2151/2011 cm^{-1}; 250 °C, 2146/2007 cm^{-1}; 260 °C, 2142/2003 cm^{-1}) and gradually decreased in intensity. No shifts occurred in the fingerprint region, and no new absorptions appeared. In the cases of **PtC$_{12}$Pt** and **PtC$_{16}$Pt**, all IR $\nu_{C\equiv C}$ bands gradually disappeared without shifting or new absorptions. The bands in the fingerprint regions were unaffected.

The title complexes were stable in air for several months. To quantitatively characterize the redox properties, cyclic voltammograms were recorded in CH_2Cl_2 under conditions used previously for dirhenium complexes such as **1**.[7, 8a,c] Data are summarized in Table 5, and typical traces are shown in Figure 2. Oxidations, presumably to the corresponding cation radicals (**II**, Scheme 1), were always observed, but no reductions took place prior to the solvent-induced limit.

Table 5. Cyclic voltammetry data.

Complex[a]	$E_{p,a}$ [V]	$E_{p,c}$ [V]	E° [V]	ΔE [mV]	$i_{c/a}$
PtC$_4$Pt	0.940	0.862	0.901	78	0.98
PtC$_8$Pt	1.261	1.143	1.202	118	0.48
PtC$_{12}$Pt	1.467	1.306	1.387	161	–
PtC$_{16}$Pt	1.514	–	–	–	–
Pt′C$_8$Pt′	1.294	1.206	1.250	88	0.52

[a] Conditions: $(7-9)\times10^{-5}$ M nBu$_4$NBF$_4$/CH_2Cl_2 at 22.5 ± 1 °C; Pt working and counter electrodes, potential vs. Ag wire pseudoreference; scan rate, 100 mV s^{-1}; ferrocene = 0.46 V.

Although none of the oxidations were chemically or electrochemically reversible, the degree of reversibility ($i_{c/a}$, ΔE) decreased dramatically with increased chain length. The oxidations also became thermodynamically less favorable (more positive E°). Given the limited stabilities of these species, no preparative experiments were attempted.

In certain cases, phosphine substitution reactions of **PtC$_x$Pt** can be used to access the "insulated" species **IV** in Scheme 1.[11] Thus, some model reactions were attempted, motivated in part by possible future mechanistic investigations. As shown in Scheme 6, **PtC$_8$Pt** or **PtC$_{12}$Pt** and excess Et_3P (1:4.3–8.0 mol ratio) were combined in CH_2Cl_2 at room temperature. Consistent with the relative phosphine donor strengths (Et_3P > p-tol$_3$P), workups gave the substitution products **Pt′C$_8$Pt′** and **Pt′C$_{12}$Pt′** in 94–90% yields. As summarized in Table 1, Table 2, Table 3, and Table 4, the thermal stabilities, IR $\nu_{C\equiv C}$ bands, ^{13}C NMR C≡C chemical shifts, and UV/Vis absorptions were very similar to those of **PtC$_8$Pt** and **PtC$_{12}$Pt**. Although square-planar d^8 complexes often exhibit associative substitution mechanisms, there is

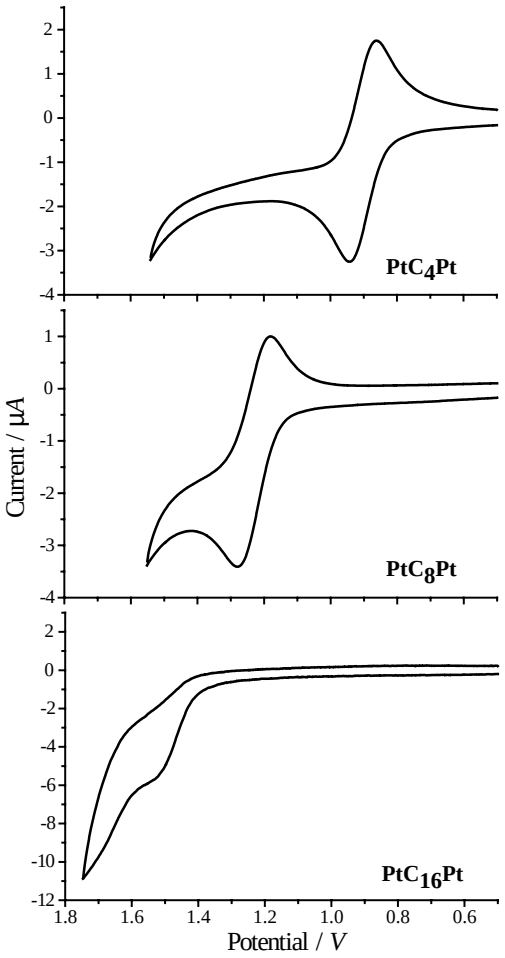

Figure 2. Representative cyclic voltammograms under the conditions of Table 5.

much precedent with platinum(II) hydrocarbyl and silyl complexes for dissociative processes.[32]

Structures: In general, the preceding compounds were easy to crystallize, and solvates were usually obtained. Accordingly, the crystal structures of **PtC$_8$Pt**, **PtC$_{12}$Pt**, **Pt′C$_{12}$Pt′**, and **PtC$_{16}$Pt** were determined as summarized in Table 6 and the Experimental Section. The molecular structures are depicted in Figure 3. All except **PtC$_{12}$Pt** exhibited a center of symmetry. Key bond lengths and angles, and other structural parameters, are presented in Table 7. Importantly, **PtC$_{16}$Pt** represents the longest polyyne crystallographically characterized to date, and only a few structures of dodecahexaynes have been determined.[4b, 9, 33, 34] The carbon chains in **PtC$_8$Pt**, **Pt′C$_{12}$Pt′**, and **PtC$_{16}$Pt** were quite linear and typical of other polyynes. However, **PtC$_{12}$Pt** exhibited a dramatic, unprecedented degree of curvature, which is analyzed together with other structural features in the Discussion Section.

We sought to quantify the relative conformations of the endgroups. Due to the various distortions from idealized platinum square planar and carbon chain geometries in this series of compounds, no single measure suffices for all purposes. In order to focus on the relative dispositions of the phosphine ligands, the following four-atom least squares planes were determined: P-Pt$_1$-P/Pt$_2$ and Pt$_1$/P-Pt$_2$-P, in which the phosphorus atoms are those directly bonded to the platinum atom specified. As summarized in Table 7, the plane-plane angles in the three molecules with centers of symmetry were 0°, as mathematically required. That in **PtC$_{12}$Pt**, 18.4°, was similar. Additional plane-plane angles involving platinum and directly ligating atoms are listed in Table 7. In the case of **PtC$_{12}$Pt**, these are much greater than 0°, due to the chain curvature.

The crystal packing was also analyzed. The complexes **Pt′C$_{12}$Pt′** and **PtC$_{16}$Pt** crystallized in motifs with parallel chains, whereas **PtC$_8$Pt** exhibited two non-parallel sets of parallel chains. Both patterns have extensive precedent with octatetraynes,[34] and a representative packing diagram is given in Figure 4. The parallel chains nearest to each other were identified, and the shortest C_{sp}-C_{sp} distance calculated (Table 7). In each case, the endgroup of one molecule nested along the carbon chain of its neighbors, as any dumbbell-shaped object would be expected to pack. Thus, the carbon chains are "offset" by ca. 1.5 atoms in **PtC$_8$Pt**, eleven atoms in **PtC$_{16}$Pt** (compare molecules in different "layers" in Figure 4), and ten atoms in **Pt′C$_{12}$Pt′**. Complex **PtC$_{12}$Pt** exhibited two perpendicular sets of "parallel" chains, as illustrated in the top portion of Figure 5. Another view of the lattice (Figure 5, bottom) shows a series of channels formed by chains of alternating curvature.

Discussion

Syntheses of title complexes: Although Scheme 2, Scheme 3, Scheme 4, and Scheme 5 contain a number of successful syntheses, they illustrate the many current challenges involved in preparing compounds with long sp carbon chains. First, there is the issue of the initial sp carbon building block. Butadiyne is easily generated and can reliably be used as a precursor to butadiynyl complexes—either directly as in Scheme 2, or via π adducts as reported for rhenium complexes.[7, 8] However, in view of the problems described above, practical procedures involving hexatriyne and octatetrayne are unlikely to be developed. Second, there is the issue of sp carbon chain extension. The C_2 species HC≡CSiEt$_3$ serves adequately in Scheme 3, but yields are moderate and 7 – 8 fold

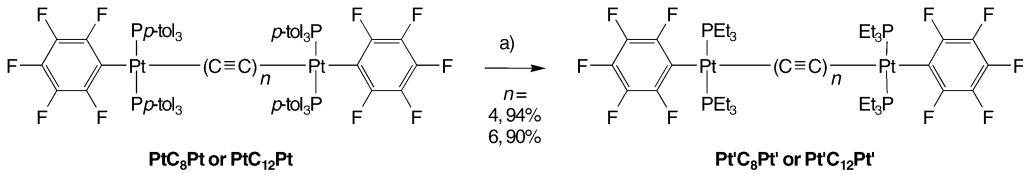

Scheme 6. Phosphine substitution reactions. a) Et$_3$P.

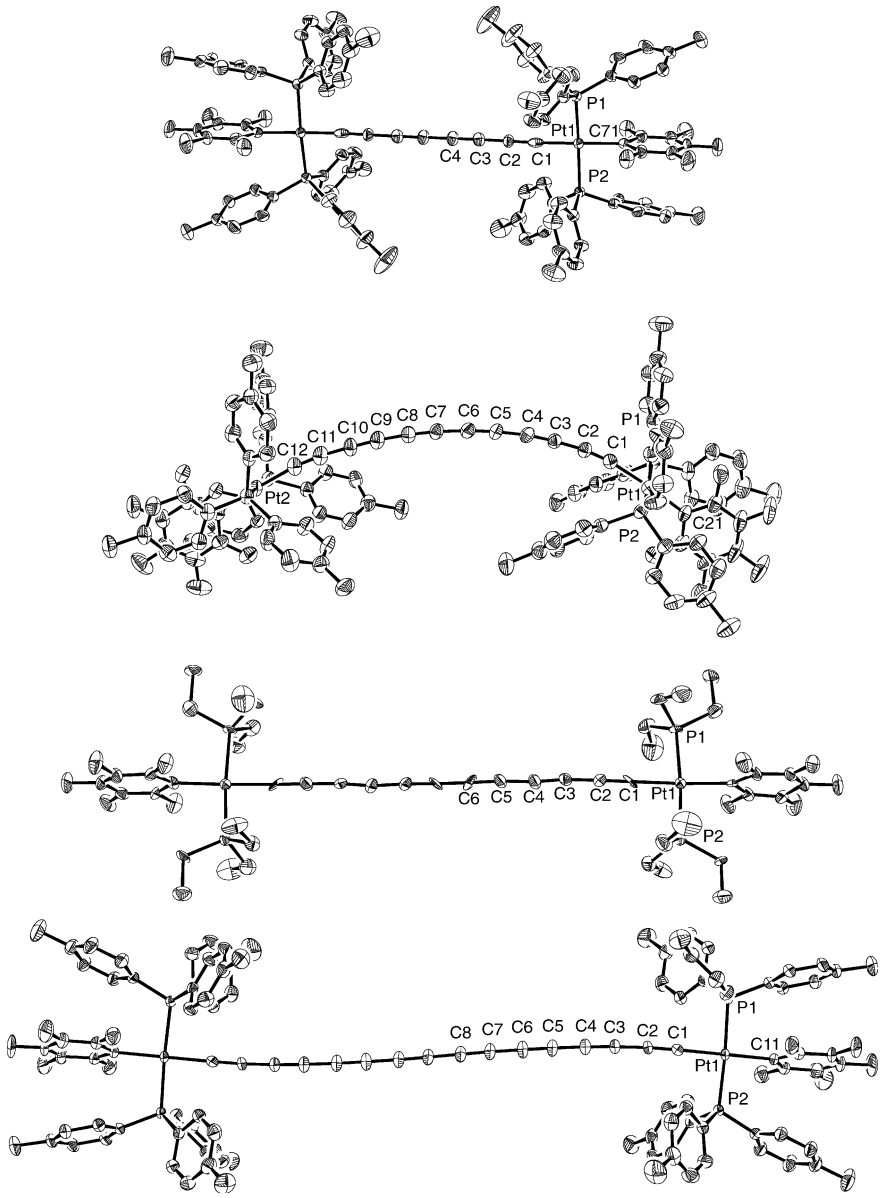

Figure 3. Structures of (from top to bottom) $\mathbf{PtC_8Pt}\cdot$(toluene), $\mathbf{PtC_{12}Pt}\cdot(\text{benzene})_4(\text{ethanol})$, $\mathbf{Pt'C_{12}Pt'}$, and $\mathbf{PtC_{16}Pt}\cdot(\text{benzene})_{10}$ with solvent molecules omitted.

excesses are necessary to minimize homocoupling of the reaction partner $\mathbf{PtC_xH}$. Efforts to use the C_4 building block $HC{\equiv}CC{\equiv}CSiMe_3$, or Cadiot–Chodkiewicz reactions, have always given inferior results with platinum pentafluorophenyl complexes.

Another challenge is the decreasing stability of $\mathbf{PtC_xH}$ with increasing chain length. While this appears to contribute to the modest yield of $\mathbf{PtC_6Pt}$ in Scheme 4, it does not seem to adversely affect the Hay oxidative homocouplings in Scheme 3. Indeed, the critical point with regard to chain extension is that the competition between homocoupling and cross-coupling with $HC{\equiv}CSiEt_3$ increasingly favors homocoupling. Accordingly, Scheme 5 represents the practical limit of our methodology. Importantly, in no cases are yields limited by the stability of $\mathbf{PtC_xPt}$. Hence, if a means can be found to increase the efficiency of cross-coupling, there is every reason to believe that the chain lengths in this series of compounds can be extended. Even at the present limit, $\mathbf{PtC_{24}Pt}$, a platinum–platinum separation of >33 Å (3.3 nm) can be calculated.

We suggest that the small quantities of $\mathbf{PtC_{20}Pt}$ generated in Scheme 3 form from the target cross-coupling product $\mathbf{PtC_{10}Si}$. The acidities of terminal alkynes increase with chain length.[29] Thus, the leaving group ability of the PtC_x moiety in $\mathbf{PtC_{10}Si}$ should be enhanced, facilitating in situ desilylation and further reaction. Accordingly, no $\mathbf{PtC_{16}Pt}$ is detected as a by-product in the conversion of $\mathbf{PtC_6H}$ to $\mathbf{PtC_8Si}$. The trace quantities of $\mathbf{PtC_{24}Pt}$ might arise by a repetition of this sequence. However, we remain open-minded with respect to alternative mechanisms, as we have occasionally encountered reactions (also in the dirhenium series **1**) that afford a puzzling distribution of chain lengths. In this context, Hirsch noted that the Hay homocoupling of an aryl-terminated $ArC_{10}H$ species gave, in addition to the desired C_{20} product, trace quantities of C_{16} and C_{18} homologues.[17b] When $ClSiMe_3$ is omitted from the homocouplings in Scheme 3, analogous species are sometimes observed.

Chain length effects; stabilities: In principle, the value of any measurable quantity for a series of conjugated polyynes can be plotted versus $1/n$, where n is the number of alkyne units. Extrapolation to the y intercept ($1/n = 0$) gives the hypothetical value for the infinite-chain species, which approximates the polyyne form of the sp carbon allotrope carbyne. Of course, many properties do not exhibit monotonic trends, and the decomposition points in Table 1 are a case in point. Nonetheless, it can confidently be predicted that some higher homologues of the title compounds should be isolable. Polyynes normally possess highly positive heats of formation, and can thus be viewed as energy-rich and thermodynamically unstable materials. We suggest that the bulk and the electropositive nature of the platinum endgroups provide steric and electronic kinetic stabilization.

Thermal sp-chain/sp-chain reactions of diynes and triynes in the solid state are well documented.[35] Cross-linked conjugated systems often form, particularly when crystal lattice properties are favorable. IR data suggest that thermolyses of

Table 6. General crystallographic data.[a]

Complex	**PtC$_8$Pt** · (toluene)	**PtC$_{12}$Pt** · (benzene)$_4$(ethanol)	**PtC$_{16}$Pt** · (benzene)$_{10}$	**Pt′C$_{12}$Pt′**
empirical formula	$C_{111}H_{92}F_{10}P_4Pt_2$	$C_{168}H_{144}F_{10}OP_4Pt_2$	$C_{172}H_{144}F_{10}P_4Pt_2$	$C_{48}H_{60}F_{10}P_4Pt_2$
formula weight	2129.91	2882.89	2914.93	1341.02
temperature [K]	173(2)	173(2)	173(2)	173(2)
wavelength [Å]	0.71073	0.71073	0.71073	0.71073
crystal system	monoclinic	monoclinic	triclinic	monoclinic
space group	$P2_1/c$	$P2_1/c$	$P\bar{1}$	$C2$
unit cell dimensions				
a [Å]	20.389(4)	19.9891(2)	15.58460(10)	14.3497(2)
b [Å]	12.114(2)	26.3139(2)	16.6860(2)	12.8955(2)
c [Å]	21.103(4)	21.9870(2)	17.1428(2)	14.5533(2)
α [°]	90	90	100.7410(10)	90
β [°]	108.32(3)	93.1800(10)	100.7620(10)	96.9509(5)
γ [°]	90	90	117.5760(10)	90
volume [Å^3]	4948.0(17)	11542.43(18)	3686.54(7)	2673.24(7)
Z	2	4	1	2
ρ_{calcd} [Mg m^{-3}]	1.430	1.659	1.313	1.666
μ [mm^{-1}]	2.954	2.558	2.002	5.412
F(000)	2128	5864	1482	1308
crystal size [mm^3]	0.35 × 0.35 × 0.15	0.30 × 0.10 × 0.05	0.35 × 0.35 × 0.35	0.40 × 0.20 × 0.15
range for data collection	1.96 to 27.47°	2.30 to 25.05°	1.93 to 27.50°	2.46 to 27.54°
index ranges	$-25 \le h \le 26$	$-23 \le h \le 23$	$-20 \le h \le 20$	$-18 \le h \le 18$
	$-14 \le k \le 15$	$-31 \le k \le 31$	$-21 \le k \le 21$	$-16 \le k \le 16$
	$-27 \le l \le 27$	$-26 \le l \le 26$	$-22 \le l \le 22$	$-18 \le l \le 18$
reflections collected	19183	40099	31770	6114
independent reflections	11299 [R(int) = 0.0454]	20382 [R(int) = 0.03941]	16857 [R(int) = 0.0213]	6114 [R(int) = 0.0000]
max. and min. transmission	0.6656 and 0.4245	0.8828 and 0.5141	0.5408 and 0.5408	0.4974 and 0.2207
data/restraints/parameters	11299/0/586	20382/1/1350	16857/0/847	6114/9/290
goodness-of-fit on F^2	1.018	1.030	1.019	1.025
final R indices [$I > 2\sigma(I)$]	$R1 = 0.0374$, $wR2 = 0.0771$	$R1 = 0.0388$, $wR^2 = 0.0911$	$R1 = 0.0273$, $wR^2 = 0.0661$	$R1 = 0.0237$, $wR^2 = 0.0600$
R indices (all data)	$R1 = 0.0675$, $wR2 = 0.0868$	$R1 = 0.0681$, $wR^2 = 0.1033$	$R1 = 0.0360$, $wR^2 = 0.0698$	$R1 = 0.0263$, $wR^2 = 0.0617$
Largest diff. peak and hole [e Å^{-3}]	1.575 and −0.840	1.198 and −0.987	1.919 and −0.939	1.185 and −1.480

[a] Features common to all structures: diffractometer, Nonius Kappa CCD; absorption correction, SCALEPACK; refinement method, full-matrix least-squares on F^2.

Table 7. Key crystallographic distances [Å] and bond or plane/plane angles [°].

	PtC$_8$Pt · (toluene)	**PtC$_{12}$Pt**[a] · (benzene)$_4$(ethanol)	**PtC$_{16}$Pt** · (benzene)$_{10}$	**Pt′C$_{12}$Pt′**
Pt–C_1	1.951(5)	1.972(6)/1.983(5)	1.981(2)	1.999(4)
$C_1 \equiv C_2$	1.252(6)	1.234(8)/1.223(7)	1.220(3)	1.205(6)
C_2–C_3	1.365(6)	1.361(8)/1.374(7)	1.355(3)	1.361(5)
$C_3 \equiv C_4$	1.209(6)	1.209(8)/1.208(7)	1.214(3)	1.224(5)
C_4–C_5 or C_4–$C_{4'}$	1.351(8)	1.363(8)/1.356(7)	1.350(3)	1.363(5)
$C_5 \equiv C_6$	–	1.216(7)/1.210(7)	1.217(4)	1.204(5)
C_6–C_7 or C_6–$C_{6'}$	–	1.358(8)	1.349(3)	1.358(7)
$C_7 \equiv C_8$	–	–	1.212(3)	–
C_8–$C_{8'}$	–	–	1.349(5)	–
$Pt_1 \cdots Pt_2$	12.895(3)	17.009(6)	23.071(4)	18.0307(3)
sum of all bond lengths from Pt_1 to Pt_2	12.905	18.067	23.145	18.070
Pt–P_1	2.3144(12)	2.3088(13)/2.3057(13)	2.3106(6)	2.309(4)
Pt–P_2	2.3063(12)	2.3129(13)/2.3071(14)	2.3136(6)	2.293(5)
Pt–C_{ipso}	2.059(4)	2.048(5)/2.058(5)	2.065(2)	2.076(3)
Pt-C_1-C_2	177.6(4)	172.9(5)/171.6(5)	175.7(2)	178.5(6)
C_1-C_2-C_3	179.2(5)	173.2(7)/171.8(6)	176.9(3)	179.3(18)
C_2-C_3-C_4	177.1(5)	178.3(7)/176.2(6)	178.2(3)	174(2)
C_3-C_4-C_5 or C_3-C_4-$C_{4'}$	178.5(6)	175.6(7)/173.4(6)	178.0(3)	173(2)
C_4-C_5-C_6	–	175.3(6)/175.3(6)	178.7(3)	176(2)
C_5-C_6-C_7 or C_5-C_6-$C_{6'}$	–	175.7(6)/175.7(6)	179.1(3)	178.4(10)
C_6-C_7-C_8	–	–	178.3(3)	–
average, Pt-C_1-C_2 and C_{sp}-C_{sp}-C_{sp}	178.1	174.6	178.0	176.5
(PPt_1P)-Pt_2 vs. (PPt_2P)-Pt_1	0	18.4	0	0
(C_{ipso}-PPt_1P) vs. (C_{ipso}-PPt_2P)	0	68.3	0	0
(C_{ipso}-PPt_1P-C_1) vs. (C_{ipso}-PPt_2P-C_1)	0	70.6	0	0
shortest C_{sp}-C_{sp} distance between parallel chains	11.936	7.535	8.786	5.353

[a] Values separated by slash are derived from the second platinum atom. The other complexes exhibit an inversion center at the midpoint of the chain.

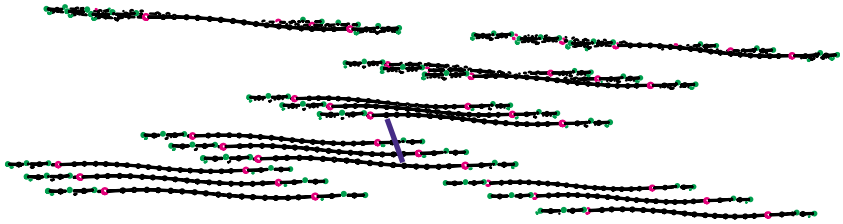

Figure 4. Packing diagram of **PtC$_{16}$Pt**·(benzene)$_{10}$ with solvent molecules and *p*-tolyl ligands omitted, and the closest sp-carbon/sp-carbon contact illustrated (8.786 Å, C1-C5′; Table 7).

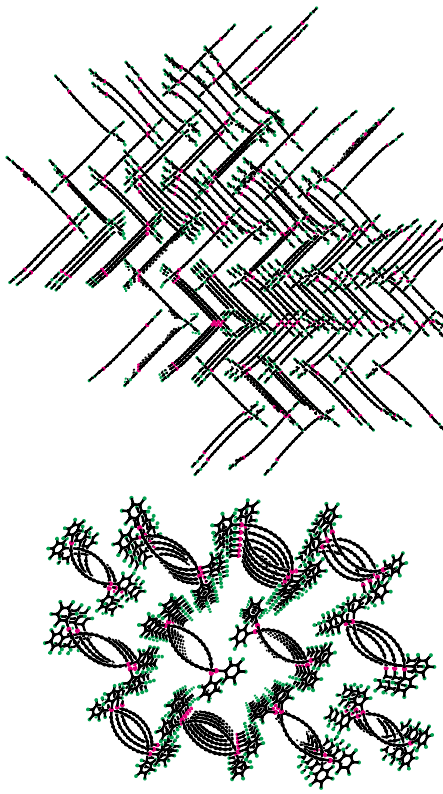

Figure 5. Packing diagrams of **PtC$_{12}$Pt**·(benzene)$_4$(ethanol), with solvent molecules and *p*-tolyl ligands omitted.

dirhenium C_x complexes such as **1** initially give new conjugated networks. However, the IR data for **PtC$_8$Pt**, **PtC$_{12}$Pt**, and **PtC$_{16}$Pt** indicate either much more extensive decomposition of the C_x moieties, or slightly modified environments en route to such decomposition.

IR and NMR spectra: The title compounds exhibit distinctive IR $\nu_{C\equiv C}$ bands, and a constant series of absorptions associated with the endgroups. The data in Table 2 show several expected trends. First, the monoplatinum complexes exhibit more bands than diplatinum complexes of the same chain length, consistent with their lower symmetry. Second, the number of bands, and the extinction coefficient of the most intense band, increase with chain length. Interestingly, **PtC$_{12}$Pt**, **Pt′C$_{12}$Pt′**, and **PtC$_{16}$Pt** exhibit one more absorption than predicted theoretically for H(C≡C)$_6$H and H(C≡C)$_8$H.[13] The vibrational spectra of polymers based upon the PtC_x repeat unit [-Pt(PR$_3$)$_2$(C≡C)$_n$-] ($n = 2$, 3) have also been analyzed in detail.[36]

The ^{31}P NMR data in Table 2 show two chain length effects. First, the chemical shifts increase monotonically from **PtC$_4$Pt** ($\delta = 16.3$ ppm) through **PtC$_{16}$Pt** ($\delta = 18.0$ ppm). The signals assigned to **PtC$_{20}$Pt** and **PtC$_{24}$Pt** ($\delta = 17.9$ and 18.2 ppm) suggest a plateau near the latter value. Second, the large $^1J_{PPt}$ coupling constants, which can be more accurately determined, decrease with chain length in every series of compounds. In the case of **PtC$_x$Pt**, plots versus $1/n$ are linear ($r = 0.99$)[37] and predict a value of 2563 Hz for **PtC$_\infty$Pt**. This trend can be assigned to small changes in hybridization in the platinum orbital used for phosphine bonding.[23] With the aryl platinum complexes *trans*-[(*p*-ZC$_6$H$_4$)Pt(PEt$_3$)$_2$X] (X = Br, H), the $^1J_{P,Pt}$ values decrease as the group Z becomes more electron-withdrawing.[38]

The ^{13}C NMR data in Table 3 show a downfield shift of the PtC≡ signal with increasing chain length in every series of compounds. In the case of **PtC$_x$Pt**, plots versus $1/n$ are again linear ($r = 0.99$)[37] and predict a value of $\delta = 116$ ppm for **PtC$_\infty$Pt**. The PtC≡*C* signals fall into a narrower range, but nonetheless always move upfield with increasing chain length. A value of $\delta = 92.8$ ppm is predicted for **PtC$_\infty$Pt**. The remaining sp carbon signals of **PtC$_8$Pt**, **PtC$_{12}$Pt**, and **PtC$_{16}$Pt** cluster between $\delta = 55.9$ and 66.7 ppm. Similar trends have been noted in all modern studies of longer polyynes.[7, 17] Hence, the ^{13}C NMR chemical shift of the polyyne form of carbyne can confidently be predicted to occur in this region.

The ^{195}Pt{^{1}H} NMR spectrum of **PtC$_8$Pt** exhibits a triplet of triplets due to coupling with two equivalent phosphorus nuclei (2651 Hz) and two equivalent *ortho* fluorine nuclei (295 Hz). Interestingly, the $J_{Pt,Pt}$ values of symmetrical diplatinum complexes can often be determined.[39] We thought that this would constitute an interesting measure of metal–metal electronic communication in **PtC$_x$Pt**. However, extensive studies with **PtC$_4$Pt** and **Pt′C$_4$Pt′**, which will be described elsewhere, showed no detectable coupling and established an upper limit of 20 Hz.[40] Longer chain lengths are certain to give still lower values.

UV/Vis spectra: As summarized in Figure 1 and Table 4, the electronic spectra of **PtC$_x$Pt** show marked chain length effects. Increasing numbers of progressively more intense bands are generally observed. From **PtC$_6$Pt** to **PtC$_{24}$Pt**, the most intense band monotonically shifts to lower energy (C_6, 315; C_8, 326; C_{12}, 359; C_{16}, 397; C_{20}, 422; C_{24}, 446 nm). For the four longest-chain compounds, this is also the longest wavelength band. For **PtC$_8$Pt**, three much weaker bands occur at longer wavelengths.[41] The extinction coefficient for **PtC$_{16}$Pt** exceeds 600 000 $M^{-1}cm^{-1}$, and those of **PtC$_{20}$Pt** and **PtC$_{24}$Pt** (Figure 1, inset) are certain to be greater still. The polyyne with the highest measured extinction coefficient prior to this study was Et$_3$Si(C≡C)$_8$SiEt$_3$ or **SiC$_{16}$Si** (336 nm, 447 000 $M^{-1}cm^{-1}$ in hexane).[15a] Hirsch has recently reported a C_{20} species with dendrimer-like aryl endgroups and a still greater value (379 nm, 604 000 $M^{-1}cm^{-1}$ in CH_2Cl_2).[17b]

With **PtC_8Si** and **PtC_8Pt**, mono- and diplatinum compounds of the same chain length can be compared. The two most intense bands of the former occur at shorter wavelengths (287, 310 nm versus 294, 326 nm), and are reversed in relative intensity. The UV/Vis spectrum of **SiC_8Si** has also been reported (Table 4).[16a] The most intense absorption shifts to still shorter wavelengths (256 nm, 195 000 $M^{-1}cm^{-1}$), although a number of very weak longer-wavelength bands are present. With **PtC_8Pt** and **$Pt'C_8Pt'$**, or **$PtC_{12}Pt$** and **$Pt'C_{12}Pt'$**, triaryl- and trialkylphosphines complexes of the same chain length can be compared. The longest wavelength bands show only modest shifts to higher energies (324 versus 314 nm; 359 versus 349 nm), indicating that the orbitals involved are only slightly affected by the phosphine.

The most intense UV/Vis bands of C_x species with various carbon, hydrogen, and trialkylsilyl endgroups, which are often but not always the longest wavelength bands, show similar chain length trends.[16, 17] These have been assigned to transitions with dominant $\pi \rightarrow \pi^*$ character, which are symmetry-allowed, in accord with the high extinction coefficients. Importantly, plots of energies versus $1/n$ ($n > 2$) are linear. Extrapolations to infinite chain length give, in all cases, values between 550 and 569 nm.[17] The dirhenium complexes represented by **1** (Scheme 1) exhibit more complicated spectra, with less intense transitions believed to have dominant $n \rightarrow \pi^*$ character at longest wavelength.[7] Nonetheless, plots of what should be the $\pi \rightarrow \pi^*$ transitions give a value of 565 nm. In the case of **PtC_xPt**, analogous plots give values of 527 nm ($x = 12$, 16, 20, 24; $r = 0.99$) or 492 nm ($x = 8$, 12, 16, 20, 24; $r = 0.97$) for **$PtC_\infty Pt$**.[37, 41b]

Given that these limiting values are so similar, a $\pi \rightarrow \pi^*$ transition at 525 – 570 nm can confidently be predicted for carbyne. In any event, all series of polyynes are predicted to have persistent, non-zero HOMO/LUMO gaps at infinite chain length. As analyzed earlier,[7, 17] this implies the convergence of C≡C and $\equiv C-C\equiv$ bond lengths to *two* distinct limiting values (*not* a common average), as supported by our structural data (analyzed below). The less intense, shorter-wavelength UV/Vis bands of **$PtC_{12}Pt$** through **$PtC_{24}Pt$** are likely due to vibrational fine structure, as observed for other polyyne families.[16, 17] The spacings in **$PtC_{20}Pt$** (1810, 1810, 1750, 1990 cm^{-1}) and **$PtC_{16}Pt$** (1910, 1800, 1770 cm^{-1}) are representative, and are close to the stretching frequencies of typical alkynes and the values in Table 2. There appears to be a trend to lower spacings at shorter chain lengths, but this is not as well-defined as in other compounds.[17a] We note in passing that the electronic spectra of many platinum alkynyl complexes have been studied in detail, and with other ligand sets a variety of additional transitions become possible.[42]

Oxidations: Although exceptions are known,[43] platinum complexes with sixteen valence electrons do not typically give chemically or electrochemically reversible oxidations.[44–46] Table 5 and Figure 2 show that the title compounds behave similarly. However, this is in one sense an advantage, as we seek to demonstrate an improved degree of reversibility with the "insulated" compounds **IV** (Scheme 1).[11] Many electrochemical oxidations of platinum alkynyl complexes have been reported,[44] including several diplatinum species with alkyne-containing unsaturated bridges.[45] Some of these feature more electron releasing donor and/or aryl ligands, which thermodynamically facilitate oxidation.[45] Most data have been interpreted in terms of successive one-electron oxidations.[43d, 45a] Hence, we believe that the voltammograms in Figure 1 reflect the formation of labile Pt^{II}/Pt^{III} mixed valence species of the type **II** (Scheme 1).

The chain length effects in Table 5 and Figure 2 parallel those found with dirhenium complexes of the type **1**.[7] First, the E° values show that oxidations become progressively less favorable thermodynamically. This should lead, from linear-free-energy considerations, to cation radicals with increased reactivity. Available evidence furthermore suggests that decomposition occurs by chain/chain coupling and/or solvent atom transfer reactions.[7] Each would be expected to become more rapid as the carbon chain lengthens and becomes less shielded by the endgroups. Together, these electronic and steric factors nicely rationalize the progressively lower degree of reversibility ($i_{c/a}$, ΔE). However, note that **PtC_4Pt** exhibits a nearly reversible couple. Surprisingly, **$Pt'C_8Pt'$** is slightly more difficult to oxidize than **PtC_8Pt**, despite a more basic or electron-releasing phosphine.

The E° values indicate that the HOMO energies decrease with chain length. At the same time, the UV/Vis data show that the $\pi \rightarrow \pi^*$ energy gaps decrease with chain length. How are these trends best reconciled? To probe these and other points, the electronic structures of PtC_xPt complexes are being examined by DFT calculations.[40] Preliminary data with the model compounds *trans,trans*-$[(C_6H_5)(H_3P)_2Pt(C{\equiv}C)_nPt(PH_3)_2(C_6H_5)]$ ($n = 2,3$) reveal the following: 1) the HOMO has substantial platinum *and* sp carbon chain character, and is of suitable symmetry of originate a $\pi \rightarrow \pi^*$ transition; 2) the HOMO energies decrease with chain length, consistent with the electrochemical data; 3) the energies of all unoccupied orbitals decrease even more with chain length, such that the HOMO/LUMO gap, and all other HOMO/unoccupied orbital spacings, decrease. Similar conclusions were reached in computational studies of C_x complexes with $[(\eta^5\text{-}C_5H_5)Fe(CO)_2]$ endgroups.[47]

Structures: Dirhenium complexes of the type **1** do not readily crystallize when the chains exceed four carbon atoms, perhaps in part because they are mixtures of diastereomers.[7, 8] As noted above, only a handful of dodecahexaynes have been structurally characterized.[4b, 9, 33, 34] Hence, the homologous series **PtC_8Pt**, **$PtC_{12}Pt$**, and **$PtC_{16}Pt$** offers a unique opportunity to examine the effect of sp carbon chain length upon molecular structure.

Since the carbon – carbon single bond of butadiyne is comprised of two sp orbitals, it is much shorter than its sp^3/sp^3 counterpart in ethane (1.384(2) versus 1.54 Å).[48] Such $\equiv C-C\equiv$ bonds contract further in conjugated polyynes.[34] As summarized in Table 7, those in the title compounds reach as low as 1.349(3) Å, a value we believe is very close to the asymptotic limit for carbyne. A computational study of **$HC_{24}H$** predicts a monotonic decrease from 1.361 to 1.339 Å as the center of the chain is approached.[13] Although the values in Table 7 suggest a similar trend, the estimated standard deviations (0.003 – 0.008 Å) preclude any conclu-

sion. The computations also predict a monotonic increase in C≡C bond lengths from 1.225 to 1.245 Å. Here, there is no discernable experimental trend. The first C≡C linkage in **PtC$_8$Pt** appears longer than the second (1.252(6) versus 1.209(6) Å), which might be rationalized as an endgroup effect. However, the difference is less in **PtC$_{16}$Pt**, and there is no significant lengthening as the center of the chain is approached (1.220(3), 1.214(3), 1.217(4), 1.212(3) Å).

The bond lengths and angles about platinum are very similar to those in monoplatinum analogues, which have been extensively analyzed elsewhere.[49] The Pt–C$_{sp}$ bond in **PtC$_{16}$Pt** is longer than that in **PtC$_8$Pt**, (1.981(2) versus 1.951(5) Å) suggesting a chain length effect. However, the Pt–C$_{sp}$ bond in the triethylphosphine complex **Pt′C$_{12}$Pt′** is longest (1.999(4) Å). As shown in Figure 3, the *p*-tol$_3$P ligands adopt conformations that create *p*-tolyl/C$_6$F$_5$/*p*-tolyl stacks, with aryl/aryl distances of 3.2–4.0 Å. Analogous motifs occur in many related complexes.[11, 22, 49b,c] These can be ascribed to attractive C$_6$F$_5$/C$_6$H$_4$ π interactions, which are now well documented in a variety of molecules.[50] This leads to nearly eclipsed *C*–*P*Pt*P*–*C* bonds. Interestingly, this feature is also found in **Pt′C$_{12}$Pt′**, which lacks the *p*-tolyl groups.

The crystal structures of **PtC$_8$Pt** and **PtC$_{16}$Pt** exhibit relatively straight chains, but **PtC$_{12}$Pt** shows a dramatic curvature (Figure 3). In contrast, **Pt′C$_{12}$Pt′** features a much straighter chain, and the related C$_{12}$ complex **3** (Scheme 1)[9] is only moderately curved. This strongly suggests that packing effects are responsible for the bending in **PtC$_{12}$Pt**. However, a detailed examination of the lattice reveals no obvious single-parameter explanation (e.g. van der Waals contacts, intermolecular π interactions, solvate molecules). DFT calculation on model alkynes show that only a few kcal mol^{-1} are needed to produce such distortions.[33b] There are also many tetraynes that crystallize, like **PtC$_{12}$Pt**, with perpendicular sets of parallel chains, but show no significant curvature.[14b, 34, 51]

We have sought to analyze this curvature in various ways. The average of the Pt-C-C and C-C-C bond angles in **PtC$_{12}$Pt**, 174.6°, is not so different from 180°, and only 1.9–3.5° less than in the other compounds in Table 7 or **3** (177.0°) However, all of the bends reinforce each other. In contrast, **PtC$_{16}$Pt** exhibits two distinct domains. From one platinum through the midpoint of the chain there is a slight curvature in one direction. Then the inversion center is crossed, leading to curvature in the opposite direction. In the case of **PtC$_{12}$Pt**, the Pt–Pt distance (17.009(6) Å) is 5.9% shorter than the sum of the intervening bond lengths (18.067 Å). With **PtC$_{16}$Pt**, the Pt–Pt distance (23.071(4) Å) is only 0.3% shorter than the sum of the intervening bond lengths (23.145 Å). In all cases but **Pt′C$_{12}$Pt′**, the Pt-C-C angle shows the greatest deviation from 180°, consistent with the lower bending force constant that would be expected.

Other polyynes show other types of deviations from linearity. However, we are unaware of any mathematically rigorous method of quantification that can be applied to all chain lengths and motifs.[34c] In our opinion, a semicircle represents a good intuitive reference point for curvature. As shown schematically in Figure 6, the Pt–Pt vector of **PtC$_{12}$Pt** defines 33.9, 30.2 and 16.6–16.7° angles, respectively, with C1, C12, and the midpoint of the chain or C6–C7 bond. If the atoms

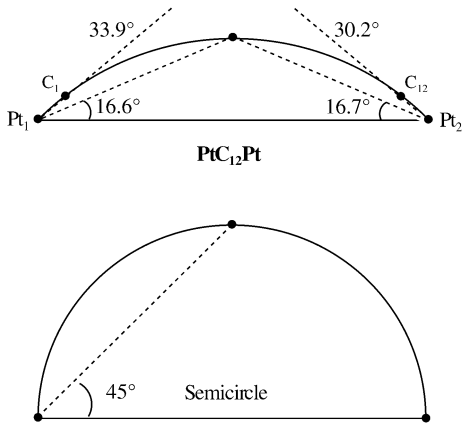

Figure 6. Comparison of chain curvature in **PtC$_{12}$Pt**·(benzene)$_4$(ethanol) with that of a semicircle.

were arrayed in a semicircle, the latter value would be 45°. Hence, the curvature in **PtC$_{12}$Pt** can be viewed as about 40% of that of a semicircle. The most highly bowed tetrayne, unsymetrically-substituted [(η^5-C$_5$Me$_5$)Re(NO)(PPh$_3$){(C≡C)$_4$-*p*-tol}], gives values of 17.1(2)° and 8.0° (ca. 18% of a semicircle).[34b] In this lattice, π-stacking interactions between *p*-tolyl groups are evident (3.0–3.5 Å distances).

The marked curvature in crystalline **PtC$_{12}$Pt** supports the speculative proposition that carbyne might easily bend and rearrange to other carbon allotropes.[14b] A final structural question involves the relative conformations of the square-planar endgroups. All of the compounds in Figure 4, and all related species reported elsewhere,[9–11] exhibit parallel or roughly parallel orientations, as best assayed by the PPtP/Pt plane-plane angles in Table 7. Preliminary DFT calculations do not show an intrinsic electronic preference for this or any other conformation.[40] Hence, it is tentatively ascribed to a lattice effect that is probably coupled to the "offset" between parallel chains noted above and exemplified for **PtC$_{16}$Pt** in Figure 4.

Conclusion

Efficient syntheses of the platinum sp carbon chain complexes **PtC$_4$Pt**, **PtC$_6$Pt**, **PtC$_8$Pt**, **PtC$_{12}$Pt**, and **PtC$_{16}$Pt** have been developed, and trace quantities of **PtC$_{20}$Pt** and **PtC$_{24}$Pt** have been generated. **PtC$_{24}$Pt** represents the longest such metal complex observed to date, **PtC$_{16}$Pt** represents the longest polyyne of any type structurally characterized to date, and **PtC$_{12}$Pt** represents the most highly curved polyyne found to date.

These complexes survive extended periods in air and heating to ≥230 °C. However, the *p*-tol$_3$P ligands are readily substituted by Et$_3$P. The IR, NMR, and UV/Vis spectra, and structural and cyclic voltammetry data, show a number of chain length effects. These help to model the properties of the one-dimensional polymeric sp carbon allotrope carbyne, which based upon this and other studies should feature alternating single and triple bonds and a non-zero HOMO/LUMO gap. The dramatic curvature in crystalline **PtC$_{12}$Pt** underscores the geometric flexibility of this allotrope.

This investigation also provides a thorough foundation for the investigation of related complexes with "insulated" sp carbon chains, as represented by **IV** in Scheme 1.[11] Parallel studies of structural, spectroscopic, thermal, and redox properties, including detailed analyses with respect to the title compounds of this work, will be described in future reports.[31, 37, 52]

Experimental Section

General: Reactions were conducted under N_2 atmospheres. Chemicals were treated as follows: hexane and THF, distilled from Na/benzophenone; acetone, distilled from P_2O_5; $HNEt_2$, distilled from KOH; TMEDA, distilled; nBu$_4$NF (trihydrate, Lancaster), dissolved in THF containing 5 wt % H_2O to give a 1.0 M solution; HC≡CSiEt$_3$, ClSiMe$_3$ (2 × Aldrich), p-tol$_3$P, Et$_3$P (2 × Fluka), CuI, CuCl (2 × Aldrich, 99.99 %), and other materials, used as received. IR and UV/Vis spectra were recorded on ASI ReactIR-1000 and Shimazu model 3102 spectrometers. NMR spectra were recorded on standard 400 MHz spectrometers. Mass spectra were recorded on a Micromass Zabspec instrument. Microanalyses were conducted on a Carlo Erba EA 1110 instrument. DSC and TGA data were recorded with a Mettler-Toledo DSC-821 instrument.[53]

***trans*-[(C$_6$F$_5$)(*p*-tol$_3$P)$_2$PtCl] (PtCl)**: A Schlenk flask was charged with [(C$_6$F$_5$)(tht)Pt(μ-Cl)]$_2$ (0.729 g, 0.750 mmol; THT = tetrahydrothiophene),[19] p-tol$_3$P (1.029 g, 3.381 mmol), and CH_2Cl_2 (25 mL). The solution was stirred for 16 h and filtered through a Celite/decolorizing carbon/glass frit assembly. Solvent was removed by rotary evaporation. The residue was washed with methanol (2 × 15 mL) and dried by oil pump vacuum to give **PtCl** as a white powder (1.410 g, 1.401 mmol, 93 %), decomp pt (capillary, onset) 230 °C. Elemental analysis calcd (%) for $C_{48}H_{42}ClF_5P_2Pt$: C 57.29, H 4.21; found: C 57.48, H 4.34; ^{1}H NMR ($CDCl_3$): δ = 7.51 (m, 12 H, o to P), 7.09 (d, $^3J_{H,H}$ = 7.8 Hz, 12 H, m to P), 2.33 ppm (s, 18 H, CH_3); ^{13}C{^{1}H} NMR:[54] δ = 145.2 (dd, $^1J_{C,F}$ = 225 Hz, $^2J_{C,F}$ = 21 Hz, o to Pt), 140.7 (s, p to P), 136.9 (dm, $^1J_{C,F}$ = 241 Hz, p to Pt), 136.2 (dm, $^1J_{C,F}$ = 245 Hz, m to Pt), 134.4 (virtual t, $^2J_{C,P}$ = 6.5 Hz, o to P), 128.7 (virtual t, $^3J_{C,P}$ = 6.0 Hz, m to P), 126.6 (virtual t, $^1J_{C,P}$ = 29.7 Hz, i to P), 114.2 (br, i to Pt), 21.3 ppm (s, CH_3); ^{31}P{^{1}H} NMR:[55] δ = 19.9 ppm (s, $^1J_{P,Pt}$ 2728 Hz); MS:[56] 1005 (**PtCl**$^+$, 5 %), 970 ([(C$_6$F$_5$)Pt(Ptol$_3$)$_2$]$^+$, 20 %), 803 ([Pt(Ptol$_3$)$_2$]$^+$, 23 %), 497 ([Pt(Ptol$_3$)]$^+$, 8 %), 304 ([Ptol$_3$]$^+$, 100 %).

***trans*-[(C$_6$F$_5$)(*p*-tol$_3$P)$_2$Pt(C≡C)$_2$H] (PtC$_4$H)**: A Schlenk flask was charged with **PtCl** (1.560 g, 1.550 mmol), CuI (0.060 g, 0.32 mmol), CH_2Cl_2 (10 mL), and $HNEt_2$ (100 mL), and cooled to −45 °C (CO_2/CH_3CN). Then butadiyne (2.9 M in THF, 8.6 mL, 24.9 mmol)[57] was added with stirring. The cold bath was allowed to warm to room temperature (ca. 3 h). After an additional 2.5 h, solvent was removed by oil pump vacuum. The residue was extracted with toluene (3 × 20 mL). The combined extracts were filtered through a neutral alumina column (7 cm, packed in toluene). Solvent was removed by rotary evaporation. The residue was washed with ethanol (20 mL) and dried by oil pump vacuum to give **PtC$_4$H** as an off-white solid (1.275 g, 1.250 mmol, 81 %), decomp pt (capillary, onset) 171 °C. Elemental analysis calcd (%) for $C_{52}H_{43}F_5P_2Pt$: C 61.24, H 4.25; found: C 60.83, H 4.31;[58] ^{1}H NMR ($CDCl_3$):[59] δ = 7.49 (m, 12 H, o to P), 7.10 (d, $^3J_{H,H}$ = 7.4 Hz, 12 H, m to P), 2.34 (s, 18 H, CH_3), 1.46 ppm (s, 1 H, ≡CH); ^{13}C{^{1}H} NMR: δ = 145.8 (dd, $^1J_{C,F}$ = 224 Hz, $^2J_{C,F}$ = 22 Hz, o to Pt), 140.7 (s, p to P), 136.8 (dm, $^1J_{C,F}$ = 239 Hz, p to Pt), 136.3 (dm, $^1J_{C,F}$ = 248 Hz, m to Pt), 134.3 (virtual t, $^2J_{C,P}$ = 6.2 Hz, o to P), 128.6 (virtual t, $^3J_{C,P}$ = 5.2 Hz, m to P), 127.4 (virtual t, $^1J_{C,P}$ = 30.2 Hz, i to P), 97.8 (s, $^1J_{C,Pt}$ = 990 Hz,[55] PtC≡C), 94.9 (s, $^2J_{C,Pt}$ = 266 Hz,[55] PtC≡C), 72.5 (s, PtC≡CC), 59.6 (s, PtC≡CC≡C), 21.3 ppm (s, CH_3); ^{19}F{^{1}H} NMR: δ = −117.31 (m, $^3J_{F,Pt}$ = 293 Hz,[55] 2 F, o to Pt), −165.07 (m, 2 F, m to Pt), −165.64 ppm (t, $^3J_{F,F}$ = 19.6 Hz, 1 F, p to Pt); MS:[56] 1020 (**PtC$_4$H**$^+$, 26 %), 970 ([(C$_6$F$_5$)Pt(Ptol$_3$)$_2$]$^+$, 72 %), 851 ([Pt(Ptol$_3$)$_2$C$_4$H]$^+$, 23 %), 803 ([Pt(Ptol$_3$)$_2$]$^+$, 100 %).

***trans*-[(C$_6$F$_5$)(*p*-tol$_3$P)$_2$Pt(C≡C)$_3$SiEt$_3$] (PtC$_6$Si)**: A three-neck flask was charged with **PtC$_4$H** (0.205 g, 0.201 mmol), HC≡CSiEt$_3$ (0.197 g, 1.40 mmol), and acetone (15 mL), and fitted with a gas dispersion tube and a condenser (cooled with circulating −20 °C ethanol). A Schlenk flask was charged with CuCl (0.050 g, 0.51 mmol) and acetone (15 mL), and TMEDA (0.030 mL, 0.20 mmol) was added with stirring. After 30 min, stirring was halted, and a green solid separated from a blue supernatant. Then O_2 was bubbled through the three-neck flask with stirring, and the solution was heated to 65 °C. After 10 min, the blue supernatant was added in portions. After 3 h, solvent was removed by rotary evaporation. The residue was extracted with hexane (3 × 5 mL) and then benzene (3 × 5 mL). The extracts were passed in sequence through a neutral alumina column (15 cm, packed in hexane). Solvent was removed from the benzene extracts by rotary evaporation and oil pump vacuum. The yellow powder was chromatographed on a silica gel column (15 cm, 10:90 v/v CH_2Cl_2/hexane to elute **PtC$_6$Si**, 40:60 v/v CH_2Cl_2/hexane to elute byproduct **PtC$_8$Pt** (0.051 g, 0.025 mmol, 25 %)). The first band was taken to dryness by oil pump vacuum to give **PtC$_6$Si** as a pale yellow powder (0.124 g, 0.107 mmol, 53 %), decomp pt (capillary, onset) 249 °C. Elemental analysis calcd (%) for $C_{60}H_{57}F_5P_2PtSi$: C 62.22, H 4.96; found: C 61.99, H 5.01;[58] ^{1}H NMR ($CDCl_3$):[59] δ = 7.45 (m, 12 H, o to P), 7.10 (d, $^3J_{H,H}$ = 7.4 Hz, 12 H, m to P), 2.36 (s, 18 H, C$_6$H$_4$CH_3), 0.90 (t, $^3J_{H,H}$ = 7.8 Hz, 9 H, CH$_2$CH_3), 0.50 ppm (q, $^3J_{H,H}$ = 7.8 Hz, 6 H, CH_2CH$_3$); ^{13}C{^{1}H} NMR:[54] δ = 146.0 (dd, $^1J_{C,F}$ = 226 Hz, $^2J_{C,F}$ = 22 Hz, o to Pt), 140.8 (s, p to P), 136.0 (dm, $^1J_{C,F}$ = 232 Hz, p to Pt), 136.3 (dm, $^1J_{C,F}$ = 248 Hz, m to Pt), 134.2 (virtual t, $^2J_{C,P}$ = 6.5 Hz, o to P), 128.7 (virtual t, $^3J_{C,P}$ = 5.5 Hz, m to P), 127.1 (virtual t, $^1J_{C,P}$ = 30.2 Hz, i to P), 104.2 (s, PtC≡C), 95.4 (s, PtC≡C), 91.2 (C≡CSi), 80.3 (s, C≡CSi), 66.1 (s, PtC≡CC), 55.9 (s, PtC≡CC≡C), 21.3 (s, C$_6$H$_4$CH_3), 7.3 (s, CH$_2$CH_3), 4.3 ppm (s, CH_2CH$_3$); MS:[56] 1158 (**PtC$_6$Si**$^+$, 2 %), 970 ([(C$_6$F$_5$)Pt(Ptol$_3$)$_2$]$^+$, 28 %), 803 ([Pt(Ptol$_3$)$_2$]$^+$, 30 %), 304 ([Ptol$_3$]$^+$, 100 %).

***trans*-[(C$_6$F$_5$)(*p*-tol$_3$P)$_2$Pt(C≡C)$_3$H] (PtC$_6$H)**: A Schlenk flask was charged with **PtC$_6$Si** (0.090 g, 0.078 mmol) and THF (25 mL). Then nBu$_4$NF (1.0 M in THF/5 wt % H_2O, 0.015 mL, 0.015 mmol) was added with stirring. After 15 min, the mixture was poured into water (40 mL) and extracted with CH_2Cl_2 (3 × 30 mL). The combined extracts were dried ($MgSO_4$), and solvent was removed by oil pump vacuum at 0 °C. The residue was extracted with cold hexane (3 × 10 mL). The extract was passed through a silica gel column (10 cm, packed in hexane) and discarded. The residue was then extracted with cold CH_2Cl_2 (1 mL). The extract was passed through the same column. The column was eluted with 10:90 v/v CH_2Cl_2/hexane. Solvent was removed from the CH_2Cl_2-containing fractions by oil pump vacuum at 0 °C to give **PtC$_6$H** as a white powder (0.069 g, 0.066 mmol, 85 %). This darkens at room temperature within a few minutes but can be stored without discolorization at −18 °C for several days.[58] ^{1}H NMR ($CDCl_3$):[59] δ = 7.45 (m, 12 H, o to P), 7.09 (d, $^3J_{H,H}$ = 7.8 Hz, 12 H, m to P), 2.34 (s, 18 H, CH_3), 1.81 (s, 1 H, ≡CH); MS:[56] 1044 (**PtC$_6$H**$^+$, 2 %), 970 ([(C$_6$F$_5$)Pt(Ptol$_3$)$_2$]$^+$, 28 %), 803 ([Pt(Ptol$_3$)$_2$]$^+$, 50 %), 304 ([Ptol$_3$]$^+$, 100 %).

***trans*-[(C$_6$F$_5$)(*p*-tol$_3$P)$_2$Pt(C≡C)$_4$SiEt$_3$] (PtC$_8$Si)**: A three-neck flask was charged with **PtC$_6$Si** (0.201 g, 0.174 mmol) and acetone (15 mL), and fitted with a gas dispersion tube and a condenser (cooled with circulating −20 °C ethanol). A Schlenk flask was charged with CuCl (0.100 g, 1.02 mmol) and acetone (30 mL), and TMEDA (0.060 mL, 0.40 mmol) was added with stirring. After 30 min, stirring was halted, and a green solid separated from a blue supernatant. Then nBu$_4$NF (1.0 M in THF/5 wt % H_2O, 0.040 mL, 0.040 mmol) was added to the solution of **PtC$_6$Si** with stirring. After 20 min, ClSiMe$_3$ (0.022 mL, 0.17 mmol) was added. Then O_2 was bubbled through the solution. The flask was transferred to a 65 °C oil bath, and HC≡CSiEt$_3$ (0.197 g, 1.40 mmol) was added, followed by portions of the blue supernatant. After 3 h, solvent was removed by rotary evaporation. The residue was extracted with hexane (3 × 5 mL) and then benzene (3 × 5 mL). The extracts were passed in sequence through a neutral alumina column (15 cm, packed in hexane). Solvent was removed from the benzene extracts by rotary evaporation. The yellow powder was chromatographed on a silica gel column (15 cm, 10:90 v/v CH_2Cl_2/hexane to elute **PtC$_8$Si**, 40:60 v/v CH_2Cl_2/hexane to elute byproduct **PtC$_{12}$Pt** (0.046 g, 0.022 mmol, 25 %)). The first band was taken to dryness by oil pump vacuum to give **PtC$_8$Si** as a pale yellow powder (0.080 g, 0.068 mmol, 39 %), decomp pt (capillary, onset) 115 °C. Elemental analysis calcd (%) for $C_{62}H_{57}F_5P_2PtSi$: C 62.99, H 4.86; found: C 62.68, H 4.80;[58] ^{1}H NMR ($CDCl_3$):[59] δ = 7.45 (m, 12 H, o to P), 7.11 (d, $^3J_{H,H}$ = 7.8 Hz, 12 H, m to P), 2.36 (s, 18 H, C$_6$H$_4$CH_3), 0.95 (t, $^3J_{H,H}$ = 7.8 Hz, 9 H, CH$_2$CH_3), 0.57 ppm (q, $^3J_{H,H}$ = 7.8 Hz, 6 H, CH_2CH$_3$); ^{13}C{^{1}H} NMR:[54] δ = 145.7 (dd, $^1J_{C,F}$ = 223 Hz, $^2J_{C,F}$ = 19 Hz, o to Pt), 140.9 (s, p to P), 140.0 (dm, $^1J_{C,F}$ = 237 Hz, p to Pt), 136.4 (dm, $^1J_{C,F}$ = 242 Hz, m to Pt), 134.2 (virtual t, $^2J_{C,P}$ = 6.5 Hz, o to P), 128.7 (virtual t, $^3J_{C,P}$ = 5.5 Hz, m to P), 126.9 (virtual t, $^1J_{C,P}$ = 30.6 Hz, i to P), 106.3 (s, $^1J_{C,Pt}$ 1000 Hz,[55] PtC≡C), 95.2 (s, $^2J_{C,Pt}$ = 264 Hz,[55] PtC≡C), 90.2 (s, C≡CSiEt$_3$), 82.9 (s, C≡CSiEt$_3$), 66.6 (s, PtC≡CC), 64.1, 59.3, 56.3 (3 s, other C≡C), 21.3 (s,

$C_6H_4CH_3$), 7.3 (s, CH_2CH_3), 4.2 ppm (s, CH_2CH_3); MS:[56] 1182 (**PtC$_8$Si**$^+$, 18%), 970 ($[(C_6F_5)Pt(Ptol_3)_2]^+$, 70%), 803 ($[Pt(Ptol_3)_2]^+$, 100%).

***trans*-[(C$_6$F$_5$)(*p*-tol$_3$P)$_2$Pt(C≡C)$_4$H] (PtC$_8$H)**: A NMR tube was charged with **PtC$_8$Si** (0.015 g, 0.013 mmol) and $CDCl_3$ (0.7 mL). Then nBu$_4$NF (1.0 M in THF/5 wt% H_2O, 0.004 mL, 0.004 mmol) was added. After 5 min the sample was analyzed by NMR and IR spectroscopy.[58] ^{1}H NMR ($CDCl_3$):[59] $\delta = 7.42$ (m, 12H, *o* to P), 7.09 (d, $^3J_{H,H} = 7.8$ Hz, 12H, *m* to P), 2.33 ppm (s, 18H, CH_3).

***trans,trans*-[(C$_6$F$_5$)(*p*-tol$_3$P)$_2$Pt(C≡C)$_2$Pt(P*p*-tol$_3$)$_2$(C$_6$F$_5$)] (PtC$_4$Pt):** A Schlenk flask was charged with **PtCl** (0.132 g, 0.131 mmol), **PtC$_4$H** (0.116 g, 0.114 mmol), CuCl (0.004 g, 0.04 mmol), and $HNEt_2$ (25 mL). The mixture was stirred for 55 h at 50 °C. After cooling, solvent was removed by oil pump vacuum, and the residue extracted with toluene (3 × 5 mL). The combined extracts were filtered through a neutral alumina column (5 cm, packed in toluene). Solvent was removed by rotary evaporation. The residue was chromatographed on a silica gel column (25 cm, 30:70 v/v CH_2Cl_2/hexane) to give **PtC$_4$Pt** as a lemon yellow solid (0.078 g, 0.039 mmol, 69%), dec pt (capillary, onset) 260 °C. Elemental analysis calcd (%) for $C_{100}H_{84}F_{10}P_4Pt_2$: C 60.36, H 4.26; found: C 60.40, H 4.49;[58] ^{1}H NMR ($CDCl_3$):[59] $\delta = 7.43$ (m, 24H, *o* to P), 6.88 (d, $^3J_{H,H} = 7.7$ Hz, 24H, *m* to P), 2.28 ppm (s, 36H, CH_3); ^{13}C{^{1}H} NMR:[54] $\delta = 145.9$ (dd, $^1J_{C,F} = 220$ Hz, $^2J_{C,F} = 22$ Hz, *o* to Pt), 139.7 (s, *p* to P), 136.5 (dm, $^1J_{C,P} = 240$ Hz, *m*/*p* to Pt), 134.4 (virtual t, $^2J_{C,P} = 6.3$ Hz, *o* to P), 128.1 (virtual t, $^1J_{C,P} = 29.7$ Hz, *i* to P), 128.1 (virtual t, $^3J_{C,P} = 5.4$ Hz, *m* to P), 104.0 (s, $^2J_{C,Pt} = 262$ Hz,[55] PtC≡*C*), 86.4 (s, $^1J_{C,Pt} = 970$ Hz,[55] Pt*C*≡C), 21.3 ppm (s, CH_3); ^{19}F{^{1}H} NMR: $\delta = -116.82$ (m, $^3J_{F,Pt} = 290$ Hz,[55] 4F, *o* to Pt), −165.54 (m, $^4J_{F,Pt} = 110$ Hz,[55] 4F, *m* to Pt), −166.61 ppm (t, $^3J_{F,F} = 19.6$ Hz, 2F, *p* to Pt); MS:[56] 1989 (**PtC$_4$Pt**$^+$, 24%), 1323 ($[(C_6F_5)Pt(Ptol_3)_3C_4]^+$, 22%), 970 ($[(C_6F_5)Pt(Ptol_3)_2]^+$, 54%), 802 ($[Pt(Ptol_3)_2\text{-}H]^+$, 72%).

***trans,trans*-[(C$_6$F$_5$)(*p*-tol$_3$P)$_2$Pt(C≡C)$_3$Pt(P*p*-tol$_3$)$_2$(C$_6$F$_5$)] (PtC$_6$Pt)**: A Schlenk flask was charged with **PtCl** (0.050 g, 0.050 mmol), $HNEt_2$ (20 mL), and CuCl (0.004 g, 0.04 mmol). The mixture was stirred until a clear solution formed and was then cooled to −45 °C. Another Schlenk flask was charged with **PtC$_6$Si** (0.048 g, 0.041 mmol) and CH_2Cl_2 (2 mL). Then nBu$_4$NF (1.0 M in THF/5 wt% H_2O, 0.010 mL, 0.010 mmol) was added. The solution was stirred for 15 min, cooled to −45 °C, and transferred via cannula to the solution of **PtCl** with stirring. The mixture was allowed to warm to room temperature. After 5 days, solvent was removed by oil pump vacuum. The residue was extracted with hexane (3 × 5 mL) and toluene (3 × 5 mL). The extracts were passed in sequence through a neutral alumina column (15 cm, packed in hexane). Solvent was removed from the toluene extracts by rotary evaporation and oil pump vacuum. The residue was chromatographed on a silica gel column (15 cm, 40:60 v/v CH_2Cl_2/hexane). The yellow band was taken to dryness by oil pump vacuum to give **PtC$_6$Pt** as a yellow powder (0.028 g, 0.014 mmol, 34%). An analytically pure sample was obtained by repeated recrystallization from $CHCl_3$/methanol, m.p. (capillary) 189 °C or (DSC, $T_i/T_e/T_p$) 178.5/184.3/189.8 °C.[53] Elemental analysis calcd (%) for $C_{102}H_{84}F_{10}P_4Pt_2$: C 60.84, H 4.20; found: 60.61, H 4.26;[58] ^{1}H NMR ($CDCl_3$):[59] $\delta = 7.44$ (m, 24H, *o* to P), 7.06 (d, $^3J_{H,H} = 7.8$ Hz, 24H, *m* to P), 2.29 ppm (s, 36H, CH_3); ^{13}C{^{1}H} NMR:[54] 145.7 (dd, $^1J_{C,F} = 226$ Hz, $^2J_{C,F} = 22$ Hz, *o* to Pt), 140.4 (s, *p* to P), 137.0 (dm, $^1J_{C,F} = 235$ Hz, *p* to Pt), 136.5 (dm, $^1J_{C,F} = 249$ Hz, *m* to Pt), 134.2 (virtual t, $^2J_{C,P} = 6.5$ Hz, *o* to P), 128.7 (virtual t, $^3J_{C,P} = 5.5$ Hz, *m* to P), 126.8 (virtual t, $^1J_{C,P} = 30.5$ Hz, *i* to P), 98.4 (s, PtC≡*C*), 95.8 (br s, Pt*C*≡C), 61.1 (s, PtC≡C*C*), 21.3 ppm (s, CH_3). MS:[56] 2014 (**PtC$_6$Pt**$^+$, 10%), 970 ($[(C_6F_5)Pt(Ptol_3)_2]^+$, 40%), 803 ($[Pt(Ptol_3)_2]^+$, 100%).

***trans,trans*-[(C$_6$F$_5$)(*p*-tol$_3$P)$_2$Pt(C≡C)$_4$Pt(P*p*-tol$_3$)$_2$(C$_6$F$_5$)] (PtC$_8$Pt)**: A three-neck flask was charged with **PtC$_4$H** (1.035 g, 1.015 mmol) and acetone (25 mL), and fitted with a gas dispersion tube and a condenser. A Schlenk flask was charged with CuCl (0.015 g, 0.15 mmol) and acetone (6 mL), and TMEDA (0.010 mL, 0.060 mmol) was added with stirring. After 30 min, stirring was halted, and a green solid separated from a blue supernatant. Then O_2 was bubbled through the three-neck flask with stirring, and the solution was heated to 65 °C. After 10 min, the blue supernatant was added in portions. After 1.5 h, solvent was removed by rotary evaporation. The residue was extracted with toluene (2 × 20 mL). The combined extracts were filtered through a neutral alumina column (7 cm, packed in toluene). Solvent was removed by rotary evaporation. Ethanol (20 mL) was added, and the yellow powder was collected by filtration and dried by oil pump vacuum to give **PtC$_8$Pt** (1.005 g, 0.493 mmol, 97%), decomp pt (capillary, gradual darkening without melting) 234 °C. Elemental analysis calcd (%) for $C_{104}H_{84}F_{10}P_4Pt_2$: C 61.30, H 4.15; found: C 61.33, H 4.12;[58] ^{1}H NMR ($CDCl_3$):[59] $\delta = 7.43$ (m, 24H, *o* to P), 7.06 (d, $^3J_{H,H} = 7.8$ Hz, 24H, *m* to P), 2.33 ppm (s, 36H, CH_3); ^{13}C{^{1}H} NMR:[54] $\delta = 145.7$ (dd, $^1J_{C,F} = 225$ Hz, $^2J_{C,F} = 22$ Hz, *o* to Pt), 140.6 (s, *p* to P), 136.8 (dm, $^1J_{C,F} = 240$ Hz, *p* to Pt), 136.6 (dm, $^1J_{C,F} = 248$ Hz, *m* to Pt), 134.2 (virtual t, $^2J_{C,P} = 6.2$ Hz, *o* to P), 128.6 (virtual t, $^3J_{C,P} = 5.4$ Hz, *m* to P), 127.2 (virtual t, $^1J_{C,P} = 30.2$ Hz, *i* to P), 100.6 (s, $^1J_{C,Pt} = 998$ Hz,[55] PtC≡C), 96.7 (s, $^2J_{C,Pt} = 265$ Hz,[55] PtC≡*C*), 64.1 (s, PtC≡C*C*), 58.1 (s, PtC≡CC≡*C*), 21.3 ppm (s, CH_3); ^{19}F{^{1}H} NMR: $\delta = -117.54$ (m, $^3J_{F,Pt} = 292$ Hz,[55] *o* to Pt), −165.31 (m, *m* to Pt), −165.89 ppm (t, $^3J_{F,F} = 19.3$ Hz, *p* to Pt); ^{195}Pt{^{1}H} NMR: $\delta = -3093$ ppm (tt, $^1J_{P,Pt} = 2651$ Hz, $^3J_{F,Pt} = 295$ Hz). MS:[56] 970 ($[(C_6F_5)Pt(Ptol_3)_2]^+$, 23%), 803 ($[Pt(Ptol_3)_2]^+$, 100%).

***trans,trans*-[(C$_6$F$_5$)(*p*-tol$_3$P)$_2$Pt(C≡C)$_6$Pt(P*p*-tol$_3$)$_2$(C$_6$F$_5$)] (PtC$_{12}$Pt)**: A three-neck flask was charged with **PtC$_6$Si** (0.100 g, 0.086 mmol) and acetone (25 mL), and fitted with a gas dispersion tube and a condenser. A Schlenk flask was charged with CuCl (0.100 g, 1.02 mmol) and acetone (30 mL), and TMEDA (0.060 mL, 0.40 mmol) was added with stirring. After 30 min, stirring was halted, and a green solid separated from a blue supernatant. Then nBu$_4$NF (1.0 M in THF/5 wt% H_2O, 0.020 mL, 0.020 mmol) was added to the solution of **PtC$_6$Si** with stirring. After 20 min, $ClSiMe_3$ (0.011 mL, 0.086 mmol) was added. Then O_2 was bubbled through the solution. After 10 min, the blue supernatant was added in portions. The flask was transferred to an oil bath, which was heated to 65 °C (ca. 10 min). After 2.2 h, solvent was removed by rotary evaporation. The residue was extracted with hexane (3 × 10 mL), which was passed through a neutral alumina column (10 cm, packed in hexane) and discarded, and then with benzene (3 × 10 mL), which was filtered through the same column. Solvent was removed by rotary evaporation. Methanol (20 mL) was added, and the yellow powder was collected by filtration and dried by oil pump vacuum to give **PtC$_{12}$Pt** (0.083 g, 0.039 mmol, 92%), decomp pt (capillary, gradual darkening without melting) 288 °C. Elemental analysis calcd (%) for $C_{108}H_{84}F_{10}P_4Pt_2$: C 62.19, H 4.06; found: C 62.27, H 4.36;[58] ^{1}H NMR ($CDCl_3$):[59] $\delta = 7.43$ (m, 24H, *o* to P), 7.09 (d, $^3J_{H,H} = 7.8$ Hz, 24H, *m* to P), 2.34 ppm (s, 36H, CH_3); ^{13}C{^{1}H} NMR:[54] $\delta = 145.7$ (dd, $^1J_{C,F} = 226$ Hz, $^2J_{C,F} = 22$ Hz, *o* to Pt), 140.9 (s, *p* to P), 136.6 (dm, $^1J_{C,F} = 240$ Hz, *p* to Pt), 136.8 ($^1J_{C,F} = 248$ Hz, *m* to Pt), 134.2 (virtual t, $^2J_{C,P} = 6.5$ Hz, *o* to P), 128.7 (virtual t, $^3J_{C,P} = 5.5$ Hz, *m* to P), 126.9 (virtual t, $^1J_{C,P} = 29.4$ Hz, *i* to P), 106.5 (s, PtC≡C), 95.5 (s, PtC≡*C*), 65.7 (s, PtC≡C*C*), 63.0, 61.0, 57.1 (3 s, other C≡C), 21.3 ppm (s, CH_3); MS:[56] 2085 (**PtC$_{12}$Pt**$^+$, 5%).

***trans,trans*-[(C$_6$F$_5$)(*p*-tol$_3$P)$_2$Pt(C≡C)$_8$Pt(P*p*-tol$_3$)$_2$(C$_6$F$_5$)] (PtC$_{16}$Pt):** A three-neck flask was charged with **PtC$_8$Si** (0.140 g, 0.119 mmol) and acetone (15 mL), and fitted with a gas dispersion tube and a condenser. A Schlenk flask was charged with CuCl (0.100 g, 1.02 mmol) and acetone (30 mL), and TMEDA (0.060 mL, 0.40 mmol) was added with stirring. After 30 min, stirring was halted and a green solid separated from the blue supernatant. Then nBu$_4$NF (1.0 M in THF/5 wt% H_2O, 0.028 mL, 0.028 mmol) was added to the solution of **PtC$_8$Si** with stirring. After 10 min, $ClSiMe_3$ (0.014 mL, 0.11 mmol) was added. Then O_2 was bubbled through the solution. After 10 min, the blue supernatant was added in portions.[60] After 1 h, solvent was removed by oil pump vacuum. The residue was extracted with hexane (3 × 15 mL), which was passed through a neutral alumina column (15 cm, packed in hexane) and discarded, and then with benzene (3 × 10 mL), which was filtered through the same column. Solvent was removed by oil pump vacuum. Methanol (20 mL) was added, and the apricot powder was collected by filtration and dried by oil pump vacuum to give **PtC$_{16}$Pt** (0.118 g, 0.055 mmol, 92%), decomp pt (capillary, gradual darkening without melting) 270 °C. Elemental analysis calcd (%) for $C_{112}H_{84}F_{10}P_4Pt_2$: C 63.04, H 3.97; found: C 62.49, H 4.16;[58] ^{1}H NMR ($CDCl_3$),[59] $\delta = 7.44$ (m, 24H, *o* to P), 7.10 (d, $^3J_{H,H} = 7.8$ Hz, 24H, *m* to P), 2.35 ppm (s, 36H, CH_3); ^{13}C{^{1}H} NMR:[54] $\delta = 145.7$ (dd, $^1J_{C,F} = 226$ Hz, $^2J_{C,F} = 22$ Hz, *o* to Pt), 141.0 (s, *p* to P), 137.0 (dm, $^1J_{C,F} = 235$ Hz, *p* to Pt), 136.5 (dm, $^1J_{C,F} = 249$ Hz, *m* to Pt), 134.2 (virtual t, $^2J_{C,P} = 6.5$ Hz, *o* to P), 128.7 (virtual t, $^3J_{C,P} = 5.5$ Hz, *m* to P), 126.8 (virtual t, $^1J_{C,P} = 30.5$ Hz, *i* to P), 109.1 (s, PtC≡C), 95.0 (s, PtC≡*C*), 66.7 (s, PtC≡C*C*), 64.9, 63.1, 61.5, 60.1, 56.8 (5 s, other C≡C), 21.3 ppm (s, CH_3). MS[56] 2133 (**PtC$_{16}$Pt**$^+$, 1%).

Attempted coupling of PtC$_8$Si and HC≡CSiEt$_3$: Complex **PtC$_8$Si** (0.140 g, 0.119 mmol), acetone (15 mL), CuCl (0.100 g, 1.02 mmol), acetone (30 mL), TMEDA (0.060 mL, 0.40 mmol), and nBu$_4$NF (1.0 M in THF/5 wt% H_2O, 0.028 mL, 0.028 mmol) were combined in a sequence analogous to that given for **PtC$_8$Si**. After 10 min, $ClSiMe_3$ (0.014 mL, 0.11 mmol) was added. Then O_2 was bubbled through the solution, and

$HC{\equiv}CSiEt_3$ (0.197 g, 1.40 mmol) was added, followed by portions of the blue supernatant.[60] After 1 h, solvent was removed by oil pump vacuum. The residue was extracted with hexane (3×15 mL), which was passed through a neutral alumina column (15 cm, packed in hexane) and discarded. The residue was then extracted with benzene (3×10 mL) and filtered through the same column. Solvent was removed by rotary evaporation. The yellow powder was chromatographed on a silica gel column (15 cm, 15:85 v/v CH_2Cl_2/hexane to elute traces of **$PtC_{10}Si$**, then 40:60 v/v CH_2Cl_2/hexane). Solvent was removed from the second band by oil pump vacuum to give a mixture of **$PtC_{16}Pt$**, **$PtC_{20}Pt$**, **$PtC_{24}Pt$** as a red powder (0.020 g). The residue was extracted with HPLC grade CH_2Cl_2. The extract was filtered through glass wool and analyzed by HPLC (11:89 v/v CH_2Cl_2/hexane on a standard silica gel column) to give the data in Table 4 and Figure 1 (typical retention times (min): **$PtC_{24}Pt$**, 30.92; **$PtC_{20}Pt$**, 43.12; **$PtC_{16}Pt$**, 66.75).

$PtC_{10}Si$: IR (powder film): $\tilde{\nu}(\nu_{C\equiv C}) = 2026$ (s), 1930 cm^{-1} (s); ^1H NMR ($CDCl_3$): $\delta = 7.43$ (m, 12 H, *o* to P), 7.10 (d, $^3J_{H,H} = 8.0$ Hz, 12 H, *m* to P), 2.34 (s, 18 H, $C_6H_4CH_3$), 0.93 (t, $^3J_{H,H} = 7.8$ Hz, 9 H, CH_2CH_3), 0.63 ppm (q, $^3J_{H,H} = 7.8$ Hz, 6 H, CH_2CH_3); $^{31}P\{^1H\}$ NMR: $\delta = 18.0$ ppm (s, $^1J_{P,Pt} = 2613$ Hz);[55] MS:[56] 1206 (**$PtC_{10}Si^+$**, 1 %), 970 ($[(C_6F_5)Pt(Ptol_3)_2]^+$, 50 %), 803 ($[Pt(Ptol_3)_2]^+$, 100 %).

Mixture of **$PtC_{16}Pt$**, **$PtC_{20}Pt$**, **$PtC_{24}Pt$** (new signals of **$PtC_{20}Pt$**, **$PtC_{24}Pt$** italicized): IR (powder film): $\tilde{\nu}(\nu_{C\equiv C}) = $ *2162* (w), *2138* (w), *2096* (m), 2057 (s), *2026* (s), 1988 cm^{-1} (s). ^1H NMR ($CDCl_3$): $\delta = 7.43$ (m, 24 H, *o* to P), 7.09 (d, $^3J_{H,H} = 7.8$ Hz, 24 H, *m* to P), 2.34 ppm (s, 36 H, CH_3); $^{13}C\{^1H\}$ NMR:[54] $\delta = 141.1$, 141.0 (2s, *p* to P), 134.2 (virtual t, $^2J_{C,P} = 6.1$ Hz, *o* to P), 128.7 (virtual t, $^3J_{C,P} = 5.5$ Hz, *m* to P), 126.8, 126.7 (virtual t, $^1J_{C,P} = 30.5$ Hz, *i* to P), 109.1 (s, Pt*C*≡C), 95.0 (s, PtC≡*C*), 66.7, 64.8, *63.4*, 63.1, *62.1*, 61.5, 60.1, 56.8 (s, other C≡C), 21.4 ppm (s, $C_6H_4CH_3$); $^{31}P\{^1H\}$ NMR: $\delta = $ *18.2*, *17.9*, 18.0 (s, $^1J_{P,Pt} = 2609$ Hz),[55] 8:77:15; MS:[56] 2182 (**$PtC_{20}Pt^+$**, 2 %), 2133 (**$PtC_{16}Pt^+$**, 5 %), 970 ($[(C_6F_5)Pt(Ptol_3)_2]^+$, 50 %), 802 ($[Pt(Ptol_3)_2\text{-}H]^+$, 100 %).

***trans,trans*-[$(C_6F_5)(Et_3P)_2Pt(C{\equiv}C)_4Pt(PEt_3)_2(C_6F_5)$] (Pt′$C_8$Pt′)**: A Schlenk flask was charged with **PtC_8Pt** (0.204 g, 0.100 mmol) and CH_2Cl_2 (40 mL). Then Et_3P (0.12 mL, 0.80 mmol) was added with stirring. After 2 h, solvent was removed by oil pump vacuum. Ethanol (10 mL) was added. The solid was collected by filtration, washed with ethanol (2×10 mL), and dried by oil pump vacuum to give **Pt′C_8Pt′** as a yellow powder (0.122 g, 0.0944 mmol, 94 %), dec pt (capillary) 189–192 °C;[58, 61] ^1H NMR ($CDCl_3$):[59] $\delta = 1.72$ (m, 24 H, CH_2), 1.04 ppm (m, 36 H, CH_3); $^{13}C\{^1H\}$ NMR:[54] 146.9 (dd, $^1J_{C,F} = 226$ Hz, $^2J_{C,F} = 22$ Hz, *o* to Pt), 137.1 (dm, $^1J_{C,F} = 245$ Hz, m/*p* to Pt), 103.4 (s, Pt*C*≡C), 91.1 (s, $^2J_{C,Pt} = 285$ Hz, PtC≡*C*), 63.9 (s, PtC≡C*C*), 57.6 (s, PtC≡CC≡*C*), 15.5 (virtual t, $^1J_{C,P} = 17.5$ Hz, CH_2), 7.7 ppm (s, CH_3); MS:[56] 1292 (**Pt′C_8Pt′**$^+$, 26 %), 598 ($[(C_6F_5)Pt(PEt_3)_2]^+$, 12 %).

***trans,trans*-[$(C_6F_5)(Et_3P)_2Pt(C{\equiv}C)_6Pt(PEt_3)_2(C_6F_5)$] (Pt′$C_{12}$Pt′)**: A Schlenk flask was charged with **$PtC_{12}Pt$** (0.118 g, 0.0566 mmol) and CH_2Cl_2 (10 mL). Then Et_3P (0.029 g (mass difference between loaded and discharged syringe), 0.24 mmol) was added with stirring. After 1 h, solvent was removed by oil pump vacuum. The residue was extracted with methanol (3×5 mL) and then CH_2Cl_2 (3×5 mL). The extracts were passed in sequence through a neutral alumina column (15 cm, packed in methanol). Solvent was removed from the CH_2Cl_2 extracts by rotary evaporation and oil pump vacuum to give **Pt′C_{12}Pt′** as a yellow powder (0.067 g, 0.051 mmol, 90 %), dec pt (capillary, onset) 270 °C;[58, 61] ^1H NMR ($CDCl_3$):[59] $\delta = 1.72$ (m, 24 H, CH_2), 1.04 ppm (m, 36 H, CH_3); $^{13}C\{^1H\}$ NMR:[54] $\delta = 146.9$ (dd, $^1J_{C,F} = 226$ Hz, $^2J_{C,F} = 22$ Hz, *o* to Pt), 137.1 (dm, $^1J_{C,F} = 245$ Hz, m/*p* to Pt), 108.1 (s, Pt*C*≡C), 90.6 (s, PtC≡*C*), 65.7 (s, PtC≡C*C*), 63.0, 61.1, 56.7 (3 s, other C≡C), 15.3 (virtual t, $^1J_{C,P} = 18.3$ Hz, CH_2), 7.7 ppm (s, CH_3); MS:[56] 1342 (**[Pt′C_{12}Pt′**+H]$^+$, 5 %).

Cyclic voltammetry: A BAS CV-50W Voltammetric Analyzer (Cell Stand C3) with the program CV-50W (version 2.0) was employed. Cells were fitted with Pt working and counter electrodes, and a Ag wire pseudoreference electrode. All CH_2Cl_2 solutions were $7-9 \times 10^{-4}$ M in substrate, 0.1 M in n-Bu_4NBF_4 (crystallized from ethanol/hexane and dried by oil pump vacuum), and prepared under nitrogen. Ferrocene was subsequently added, and calibration voltammograms recorded. The ambient laboratory temperature was 22.5 ± 1 °C.

Crystallography: **A**: Ethanol vapor was allowed to diffuse into a toluene solution of **PtC_8Pt** at room temperature. After one week, the thin yellow plates of **PtC_8Pt**·(toluene) had formed, and data were collected as outlined in Table 5. Cell parameters were obtained from 10 frames using a 10° scan and refined with 37010 reflections. Lorentz, polarization, and absorption corrections[62] were applied. The space group was determined from systematic absences and subsequent least-squares refinement. The structure was solved by direct methods. The parameters were refined with all data by full-matrix-least-squares on F^2 using SHELXL-97.[63] Non-hydrogen atoms were refined with anisotropic thermal parameters. The hydrogen atoms were fixed in idealized positions using a riding model. Scattering factors were taken from literature.[64] The asymmetric unit contained a half molecule of disordered toluene. **B**: Ethanol vapor was allowed to diffuse into a benzene solution of **$PtC_{12}Pt$** at room temperature. After one week, the thin yellow needles of **$PtC_{12}Pt$**·$(benzene)_4$(ethanol) had formed, and data were collected and refined as in A (cell parameters from 20768 reflections). The asymmetric unit contained four molecules of benzene and one of disordered ethanol. **C**: Ethanol vapor was allowed to diffuse into a benzene solution of **$PtC_{16}Pt$** at room temperature. After one week, the thin orange needles of **$PtC_{16}Pt$**·$(benzene)_{10}$ had formed, and data were collected and refined as in A (cell parameters from 16192 reflections). The unit cell contained ten benzene molecules. **D**: A CH_2Cl_2 solution of **Pt′C_{12}Pt′** was allowed to slowly evaporate. After one week, yellow prisms had formed, and data were collected and refined as in A (cell parameters from 3204 reflections). The structure was refined as a racemic twin with a 52:48 ratio (Flack parameter: 0.520(15)).[65]

Acknowledgement

We thank the Deutsche Forschungsgemeinschaft (GL 300/1-2) and Johnson Matthey PMC (platinum loan) for support, and Dr. Fedor Zhuravlev for helpful discussions.

[1] References 2–11 are limited to C_8 complexes and higher homologues. Reviews of C_x complexes: a) M. I. Bruce, *Coord. Chem. Rev.* **1997**, *166*, 91; b) F. Paul, C. Lapinte in *Unusual Structures and Physical Properties in Organometallic Chemistry* (Eds.: M. Gielen, R. Willem, B. Wrackmeyer), Wiley, New York, **2002**, chap. 6; c) See also P. J. Low, M. I. Bruce, *Adv. Organomet. Chem.* **2001**, *48*, 71.

[2] a) F. Coat, C. Lapinte, *Organometallics* **1996**, *15*, 477; b) F. Coat, P. Thominot, C. Lapinte, *J. Organomet. Chem.* **2001**, *629*, 39.

[3] a) M. I. Bruce, M. Ke, P. J. Low, B. W. Skelton, A. H. White, *Organometallics* **1998**, *17*, 3539; b) M. I. Bruce, B. D. Kelly, B. W. Skelton, A. H. White, *J. Organomet. Chem.* **2000**, *604*, 150.

[4] a) M. Akita, M.-C. Chung, A. Sakurai, S. Sugimoto, M. Terada, M. Tanaka, Y. Moro-oka, *Organometallics* **1997**, *16*, 4882; b) A. Sakurai, M. Akita, Y. Moro-oka, *Organometallics* **1999**, *18*, 3241; c) M. Akita, A. Sakurai, Y. Moro-oka, *Chem. Commun.* **1999**, 101.

[5] K.-T. Wong, J.-M. Lehn, S.-M. Peng, G.-H. Lee, *Chem. Commun.* **2000**, 2259.

[6] P. J. Kim, H. Masai, K. Sonogashira, N. Hagihara, *Inorg. Nucl. Chem. Lett.* **1970**, *6*, 181.

[7] R. Dembinski, T. Bartik, B. Bartik, M. Jaeger, J. A. Gladysz, *J. Am. Chem. Soc.* **2000**, *122*, 810.

[8] a) W. E. Meyer, A. J. Amoroso, C. R. Horn, M. Jaeger, J. A. Gladysz, *Organometallics* **2001**, *20*, 1115; b) C. R. Horn, J. M. Martín-Alvarez, J. A. Gladysz, *Organometallics* **2002**, *21*, 5386; c) C. R. Horn, J. A. Gladysz, *Eur. J. Inorg. Chem.* **2003**, in press..

[9] T. B. Peters, J. C. Bohling, A. M. Arif, J. A. Gladysz, *Organometallics* **1999**, *18*, 3261. The C_{16} analogue of **3** (Scheme 1) will be described in the full paper corresponding to this communication.

[10] W. Mohr, J. Stahl, F. Hampel, J. A. Gladysz, *Inorg. Chem.* **2001**, *40*, 3263.

[11] J. Stahl, J. C. Bohling, E. B. Bauer, T. B. Peters, W. Mohr, J. M. Martín-Alvarez, F. Hampel, J. A. Gladysz, *Angew. Chem.* **2002**, *114*, 1951; *Angew. Chem. Int. Ed.* **2002**, *41*, 1871.

[12] Additional relevant papers from our laboratory or Lapinte's: a) T. Bartik, W. Weng, J. A. Ramsden, S. Szafert, S. B. Falloon, A. M. Arif, J. A. Gladysz, *J. Am. Chem. Soc.* **1998**, *120*, 11071; b) S. B. Falloon, S. Szafert, A. M. Arif, J. A. Gladysz, *Chem. Eur. J.* **1998**, *4*, 1033; c) F. Paul, W. E. Meyer, L. Toupet, H. Jiao, J. A. Gladysz, C. Lapinte, *J. Am. Chem. Soc.* **2000**, *122*, 9405.

[13] L. Horný, N. D. K. Petraco, C. Pak, H. F. Schaefer III, *J. Am. Chem. Soc.* **2002**, *124*, 5861.

[14] a) V. M. Mel'nichenko, A. M. Sladkov, Yu. N. Nikulin, *Russ. Chem. Rev.* **1982**, *51*, 421; b) R. J. Lagow, J. J. Kampa, H.-C. Wei, S. L. Battle, J. W. Genge, D. A. Laude, C. J. Harper, R. Bau, R. C. Stevens, J. F. Haw, E. Munson, *Science* **1995**, *267*, 362; c) Yu. P. Kudryavtsev, R. B. Heimann, S. E. Evsyukov, *J. Mater. Sci.* **1996**, *31*, 5557; d) F. Cataldo, *Polym. Int.* **1997**, *44*, 191; e) K.-H. Homann, *Angew. Chem.* **1998**, *110*, 2572; *Angew. Chem. Int. Ed.* **1998**, *37*, 2434; f) J. Hlavatý, L. Kavan, N. Kasahara, A. Oya, *Chem. Commun.* **2000**, 737.

[15] a) J. A. McCleverty, M. D. Ward, *Acc. Chem. Res.* **1998**, *31*, 842; b) J.-P. Launay, C. Coudret in *Electron Transfer in Chemistry*, *Vol. 5*, Part 1 (Ed.: V. Balzani), Wiley-VCH, Weinheim, **2001**, chap. 1; c) L. De Cola, P. Belser in *Electron Transfer in Chemistry*, *Vol. 5*, Part 1 (Ed.: V. Balzani), Wiley-VCH, Weinheim, **2001**, chap. 3; d) F. Scandola, C. Chiorboli, M. T. Indelli, M. A. Rampi in *Electron Transfer in Chemistry*, *Vol. 3*, Part 2 (Ed.: V. Balzani), Wiley-VCH, Weinheim, **2001**, chap. 3; e) R. L. Carrol, C. B. Gorman, *Angew. Chem.* **2002**, *114*, 4556; *Angew. Chem. Int. Ed.* **2002**, *41*, 4378.

[16] Older studies featuring *tert*-butyl or trialkylsilyl endgroups: a) R. Eastmond, T. R. Johnson, D. R. M. Walton, *Tetrahedron* **1972**, *28*, 4601; b) T. R. Johnson, D. R. M. Walton, *Tetrahedron* **1972**, *28*, 5221.

[17] Modern studies featuring cyano or dendrimer-like aryl endgroups: a) G. Schermann, T. Grösser, F. Hampel, A. Hirsch, *Chem. Eur. J.* **1997**, *3*, 1105; b) T. Gibtner, F. Hampel, J.-P. Gisselbrecht, A. Hirsch, *Chem. Eur. J.* **2002**, *8*, 408.

[18] For other $[(C_6F_5)(L)_2PtC{\equiv}CR]$ systems, see the following recent papers and references therein: a) L. R. Falvello, J. Forniés, J. Gómez, E. Lalinde, A. Martín, F. Martínez, M. T. Moreno, *J. Chem. Soc. Dalton Trans.* **2001**, 2132; b) J. R. Berenguer, J. Forniés, E. Lalinde, A. Martín, B. Serrano, *J. Chem. Soc. Dalton Trans.* **2001**, 2926.

[19] R. Usón, J. Forniés, P. Espinet, G. Alfranca, *Synth. React. Inorg. Met.-Org. Chem.* **1980**, *10*, 579.

[20] R. Usón, J. Forniés, P. Espinet, R. Navarro, C. Fortuño, *J. Chem. Soc. Dalton Trans.* **1987**, 2077.

[21] We find $[\{(C_6F_5)Pt(tht)(\mu\text{-}Cl)\}_2]$ to be a 72:28 mixture of isomers in $CDCl_3$, as assayed by ^{19}F NMR. These differ in the *cis*/*trans* sense of the THT ligands on opposite platinum atoms, as observed with several closely related compounds: P. Espinet, J. M. Martínez-Ilarduya, C. Pérez-Briso, A. L. Casado, M. A. Alonso, *J. Organomet. Chem.* **1998**, *551*, 9.

[22] J. Ruwwe, J. M. Martín-Alvarez, C. R. Horn, E. B. Bauer, S. Szafert, T. Lis, F. Hampel, P. C. Cagle, J. A. Gladysz, *Chem. Eur. J.* **2001**, *7*, 3931.

[23] P. S. Pregosin, L. M. Venanzi, *Chem. Br.* **1978**, 276.

[24] a) U. Niedballa, in *Methoden der Organischen Chemie*, *Vol. V/2a (Houben-Weyl)* (Ed.: E. Müller), Georg Thieme, Stuttgart, **1977**, p. 917; b) W. Hunsmann, *Chem. Ber.* **1950**, *83*, 213.

[25] Y. Rubin, S. S. Lin, C. B. Knobler, J. Anthony, A. M. Boldi, F. Diederich, *J. Am. Chem. Soc.* **1991**, *113*, 6943.

[26] W. Weng, T. Bartik, M. Brady, B. Bartik, J. A. Ramsden, A. M. Arif, J. A. Gladysz, *J. Am. Chem. Soc.* **1995**, *117*, 11922.

[27] P. Siemsen, R. C. Livingston, F. Diederich, *Angew. Chem.* **2000**, *112*, 2740; *Angew. Chem. Int. Ed.* **2000**, *39*, 2632.

[28] When the prior isolation of crude $\mathbf{PtC_8H}$ was attempted, or the addition of $ClSiMe_3$ omitted, only small quantities of $\mathbf{PtC_{16}Pt}$ were obtained. Mass spectra of the product mixture also showed ions for $\mathbf{PtC_{10}Pt}$ and $\mathbf{PtC_{12}Pt}$.

[29] R. Eastmond, T. R. Johnson, D. R. M. Walton, *J. Organomet. Chem.* **1973**, *50*, 87.

[30] a) K. Sonogashira, T. Yatake, Y. Tohda, S. Takahashi, N. Hagihara, *J. Chem. Soc. Chem. Commun.* **1977**, 291; b) K. Sonogashira, Y. Fujikura, T. Yatake, N. Toyoshima, S. Takahashi, N. Hagihara, *J. Organomet. Chem.* **1978**, *145*, 101.

[31] J. Stahl, Doctoral Thesis, Universität Erlangen-Nürnberg, in preparation.

[32] a) O. F. Wendt, R. J. Deeth, L. I. Elding, *Inorg. Chem.* **2000**, *39*, 5271, and references therein; b) M. R. Plutino, L. M. Scolaro, R. Romeo, A. Grassi, *Inorg. Chem.* **2000**, *39*, 2712, and references therein.

[33] a) R. D. Adams, B. Qu, M. D. Smith, *Organometallics* **2002**, *21*, 3867; b) J. Classen, R. Gleiter, F. Rominger, *Eur. J. Inorg. Chem.* **2002**, 2040.

[34] Crystallographically characterized 1,3,5,7-tetraynes and higher polyynes are summarized in these papers: a) B. Bartik, R. Dembinski, T. Bartik, A. M. Arif, J. A. Gladysz, *New J. Chem.* **1997**, *21*, 739; b) R. Dembinski, T. Lis, S. Szafert, C. L. Mayne, T. Bartik, J. A. Gladysz, *J. Organomet. Chem.* **1999**, *578*, 229; c) S. Szafert, J. A. Gladysz, *Chem. Rev.*, submitted.

[35] For a lead reference to an extensive literature, see J. Xiao, M. Yang, J. W. Lauher, F. W. Fowler, *Angew. Chem.* **2000**, *112*, 2216; *Angew. Chem. Int. Ed.* **2000**, *39*, 2132.

[36] R. D. Markwell, I. S. Butler, A. K. Kakkar, M. S. Khan, Z. H. Al-Zakwani, J. Lewis, *Organometallics* **1996**, *15*, 2331.

[37] W. Mohr, Doctoral Thesis, Universität Erlangen-Nürnberg, **2002**.

[38] D. P. Arnold, M. A. Bennett, *Inorg. Chem.* **1984**, *23*, 2117.

[39] D. Carmona, R. Thouvenot, L. M. Venanzi, F. Bachechi, L. Zambonelli, *J. Organomet. Chem.* **1983**, *250*, 589.

[40] F. Zhuravlev, unpublished results, Universität Erlangen-Nürnberg.

[41] A reviewer has raised some thoughtful points concerning the UV/Vis data. a) One issue is whether the weaker, longer wavelength bands of $\mathbf{PtC_8Pt}$ and $\mathbf{Pt'C_8Pt'}$ (Table 4; their ε values are too low to be seen in Figure 1) might be artifacts. Solvent impurities can be excluded, since they are absent in other spectra recorded with the same solvent sample. Such bands are furthermore observed in other octatetraynes, such as $\mathbf{SiC_8Si}$ (in both methanol and hexane; see Table 4).[16a] In higher homologues such as $\mathbf{PtC_{12}Pt}$ and $\mathbf{PtC_{16}Pt}$, the analogous bands might be obscured by the increasingly intense visible absoprtions. Although these weak transitions are clearly of interest, further analysis is beyond the scope of the present study. b) To estimate the energy of the $\pi \rightarrow \pi^*$ transition for $\mathbf{PtC_\infty Pt}$, the same v/v′ transitions of $\mathbf{PtC_x Pt}$ must be compared. In cognizance of this issue, only data for $\mathbf{PtC_8Pt}$ and higher homologues—where abrupt changes would be less likely, the $\pi \rightarrow \pi^*$ transitions can be assigned with good confidence, and endgroup effects play a smaller role—have been utilized.

[42] a) H. Masai, K. Sonogashira, N. Hagihara, *Bull. Chem. Soc. Jpn.* **1971**, *44*, 2226; b) M. Hissler, W. B. Connick, D. K. Geiger, J. E. McGarrah, D. Lipa, R. J. Lachicotte, R. Eisenberg, *Inorg. Chem.* **2000**, *39*, 447, and references therein; c) V. W.-W. Yam, *Acc. Chem. Res.* **2002**, *35*, 555, and references therein.

[43] Leading references: a) A. M. Bond, R. Colton, D. A. Fiedler, J. E. Kevekordes, V. Tedesco, T. F. Mann, *Inorg. Chem.* **1994**, *33*, 5761; b) J. Forniés, B. Menjón, R. M. Sanz-Carillo, M. Tomás, N. G. Connelly, J. G. Crossley, A. G. Orpen, *J. Am. Chem. Soc.* **1995**, *117*, 4295; c) A. Klein, W. Kaim, *Organometallics* **1995**, *14*, 1176; d) A. Klein, S. Hasenzahl, W. Kaim, J. Fiedler, *Organometallics* **1998**, *17*, 3532.

[44] a) V. W.-W. Yam, R. P.-L. Tang, K. M.-C. Wong, K.-K. Cheung, *Organometallics* **2001**, *20*, 4476, and references therein; b) J. E. McGarrah, Y.-J. Kim, M. Hissler, R. Eisenberg, *Inorg. Chem.* **2001**, *40*, 4510, and references therein.

[45] a) M. Younus, A. Köhler, S. Cron, N. Chawdhury, M. R. A. Al-Mandhary, M. S. Khan, J. Lewis, N. J. Long, R. H. Friend, P. R. Raithby, *Angew. Chem.* **1998**, *110*, 3180; *Angew. Chem. Int. Ed.* **1998**, *37*, 3036; b) S. Back, M. Lutz, A. L. Spek, H. Lang, G. van Koten, *J. Organomet. Chem.* **2001**, *620*, 227, and references therein.

[46] M. Sato, A. Asami, G. Maruyama, M. Kosuge, J. Nakayama, S. Kumakura, T. Fujihara, K. Unoura, *J. Organomet. Chem.* **2002**, *654*, 56.

[47] P. Belanzoni, N. Re, A. Sgamellotti, C. Floriani, *J. Chem. Soc. Dalton Trans.* **1998**, 1825.

[48] M. Tanimoto, K. Kuchitsu, Y. Morino, *Bull. Chem. Soc. Jpn.* **1971**, *44*, 386.

[49] a) J. C. Bohling, T. B. Peters, A. M. Arif, F. Hampel, J. A. Gladysz in *Coordination Chemistry at the Turn of the Century* (Eds.: G. Ondrejovic, A. Sirota) Slovak Technical University Press, Bratislava, Slovakia, **1999**, pp. 47–52; b) T. B. Peters, Q. Zheng, J. Stahl, J. C. Bohling, A. M. Arif, F. Hampel, J. A. Gladysz, *J. Organomet. Chem.* **2002**, *641*, 53; c) W. Mohr, T. B. Peters, J. C. Bohling, F. Hampel, A. M. Arif, J. A. Gladysz, *C. R. Chim.* **2002**, *5*, 111.

[50] a) H. Adams, J.-L. Jimenez Blanco, G. Chessari, C. A. Hunter, C. M. R. Low, J. M. Sanderson, J. G. Vinter, *Chem. Eur. J.* **2001**, *7*, 3494; b) J. C. Collings, K. P. Roscoe, R. Ll. Thomas, A. S. Batsanov, L. M. Stimson, J. A. K. Howard, T. B. Marder, *New J. Chem.* **2001**, *25*, 1410; c) A. F. M. Kilbinger, R. H. Grubbs, *Angew. Chem.* **2002**, *114*, 1633; *Angew. Chem. Int. Ed.* **2002**, *41*, 1563.

[51] B. F. Coles, P. B. Hitchcock, D. R. M. Walton, *J. Chem. Soc. Dalton Trans.* **1975**, 442.

[52] J. Stahl, E. B. Bauer, W. Mohr, F. Hampel, J. A. Gladysz, unpublished results.
[53] For the definition of parameters employed, see: H. K. Cammenga, M. Epple, *Angew. Chem.* **1995**, *107*, 1284; *Angew. Chem. Int. Ed. Engl.* **1995**, *34*, 1171.
[54] The signal of the *ipso* C_6F_5 carbon was not observed.
[55] This coupling represents a satellite (d; $^{195}Pt = 33.8\,\%$), and is not reflected in the peak multiplicity given.
[56] *m*/*z* (FAB, 3-NBA) for the most intense peak of the isotope envelope. For some compounds, the most strongest signal is matrix-derived and no ion of 100% intensity is specified.
[57] The butadiyne concentration is calculated from the mass increase of the THF solution. **CAUTION**: this explosive compound was generated and handled as described in L. Brandsma, H. D. Verkruijsse, *Synthesis of Acetylenes, Allenes and Cumulenes*, Elsevier, New York, **1981**, p. 146.
[58] For TGA, IR, and/or UV/Vis data, see Tables 1, 2 and 4.
[59] For ^{31}P NMR data, see Table 2.
[60] The initial addition was ca. 14 mL (for this homocoupling, lesser amounts appeared to generate a precipitate). Then several smaller portions were added until ca. 20 mL was reached.
[61] A satisfactory microanalysis was not obtained for this compound.
[62] a) "Collect" data collection software, B. V. Nonius **1998**; b) "Scalepack" data processing software: Z. Otwinowski, W. Minor, *Methods Enzymol.* **1997**, *276*, 307 (Macromolecular Crystallography, Part A).
[63] G. M. Sheldrick, SHELX-97, Program for refinement of crystal structures, University of Göttingen, Göttingen (Germany), **1997**.
[64] D. T. Cromer, J. T. Waber in *International Tables for X-ray Crystallography* (Eds.: J. A. Ibers, W. C. Hamilton), Kynoch, Birmingham, **1974**.
[65] H. D. Flack, *Acta Crystallogr. Sect. A* **1983**, *39*, 876.

Received: January 17, 2003 [F4741]